Evaluation of the effects of shrinkage stress of dental composites with different filling techniques

PhD Thesis

Dr. Viktória Néma

Supervisors:

Dr. habil Edina Lempel

Dr. habil Márk Fráter

University of Szeged

Doctoral School of Clinical Medicine

Szeged, Hungary

2024

1. Table of contents

2. List of the publications providing the basis of, and related to the topic of the thesis

Publications providing the basis of the thesis:

Néma V; Sáry T; Szántó LF; Braunitzer G; Fráter M: Rövid üvegszál megerősítésű kompozit által kifejtett polimerizációs stressz. Előzetes tanulmány [Polymerization shrinkage-stress of short fiber-reinforced composite. Pilot study]. FOGORVOSI SZEMLE, 115 (4). pp. 178-182. ISSN 0015-5314 (2022)

Néma V, Sáry T, Szántó FL, Szabó B, Braunitzer G, Lassila L, Garoushi S, Lempel E, Fráter M. Crack propensity of different direct restorative procedures in deep MOD cavities. Clin Oral Investig. 2023 May;27(5):2003-2011. doi: 10.1007/s00784-023-04927-1.
IF: 3.4 (2022) Q1, D1

Néma V, Kunsági-Máté S, Őri Z, Kiss T, Szabó P, Szalma J, Fráter M, Lempel E. Relation between internal adaptation and degree of conversion of short-fiber reinforced resin composites applied in bulk or layered technique in deep MOD cavities. Dent Mater. 2024 Feb 16:S0109-5641(24)00030-7. doi: 10.1016/j.dental.2024.02.013.
IF: 5 (2022) Q1, D1

Related publication:

Fráter M, Sáry T, **Néma V**, Braunitzer G, Vallittu P, Lassila L, Garoushi S. Fatigue failure load of immature anterior teeth: influence of different fiber post-core systems. Odontology. 2021 Jan;109(1):222-230. doi: 10.1007/s10266-020-00522-y.

3. List of Abbreviations

- RBC: resin-based composite
- SFRC: short fiber-reinforced resin composite
- DC: degree of conversion
- PMMA: polymethyl methacrylate
- BisGMA: bisphenol-A glycidyl dimethacrylate
- CP: closed pore
- IA: internal adaptation
- IG%: interfacial gap percentage
- micro-CT: micro-computed tomography
- MOD: mesio-occluso-distal
- ROI: region of interest
- SEM: scanning electron microscopy
- semi-IPN: semi-interpenetrating polymer network
- TEGDMA: triethylene glycol dimethacrylate

4. Introduction

Dental resin-based composites (RBCs) are the most frequently used direct restorative materials and have become the first choice for the majority of practitioners worldwide for restoring both anterior and posterior teeth (1). Direct composite fillings are among the most performed medical treatments, with more than five hundred million composite restorations placed worldwide annually (2).

In a comprehensive review of clinical outcome studies, Manhart and colleagues found an average annual failure rate of 1-3% for direct posterior RBCs (3). The primary causes of failure in posterior restorations are secondary caries and fractures, with survival rates of 70-98% after 8 and 22 years (4, 5). Bernardo et al. (6) observed an acceleration in the annual failure rate from 0.95% for single-surface restorations to 9.43% for restorations with four or more surfaces. Thus, the larger the restorations, the greater the tendency for failure due to mechanical, fracture-related problems, leading to reduced longevity (7). Lempel et al. found an acceptable clinical performance for direct anterior composite resin restorations, with an annual failure rate as low as 1.43% after an average follow-up period of 7.2 years. The causes of failure included fractures or chipping of the restoration and color mismatch (8). Secondary caries is thought to be induced indirectly by polymerization shrinkage (9) and restoration fractures, both of which remain the main problems to be overcome (10). While monomers can be directly responsible for the bulk shrinkage of materials, filler loading and certain filler technologies have been shown to reduce bulk shrinkage and hence help minimize this problem (11). During the restorative process, non-functional stress effects may occur, increasing the total stress intensity and leading to the potential for early structural failure of the tooth structure, the restoration, or the tooth-restoration interface. The dimensional change in restorative materials, which causes internal stresses in the restored tooth structure, is a major source of non-functional stresses. As dimensional changes are common in most restorative materials during the setting reactions or when water is absorbed in the moist oral milieu, understanding the dynamics and effects of these changes is of paramount importance for the clinical performance of restorative materials (12, 13). This will be emphasized throughout this thesis.

1.1 Dental resin-based composites (RBC)

The composition of dental RBCs has significantly improved over the last decades since these materials were first introduced into dentistry (14). RBCs have four major constituents: an organic polymer matrix, inorganic filler particles, a coupling agent, and the initiator-accelerator system (15). The predominant base monomers used for the resin matrix are dimethacrylate compounds. The most commonly used monomer is the high-viscosity 2,2-bis[4(2-hydroxy-3-methacryloxypropyloxy)phenyl]propane (Bis-GMA), which is blended with a lower molecular weight monomer, triethylene glycol dimethacrylate (TEGDMA), to reduce viscosity. Another commonly used base monomer is the low-viscosity, highly flexible urethane dimethacrylate (UDMA), which has been found to be more reactive than Bis-GMA (16). These dimethacrylate monomers contain reactive carbon double bonds at both ends that can be subjected to initiator-induced radical addition polymerization (14, 15). The dispersed inorganic filler particles can be silica, zirconia, or glass-ceramic, either spherical or irregular in shape, with sizes ranging from micrometers to nanometers. The coupling agent, an organosilane (often referred to as silane), is applied by the manufacturer to the inorganic particles for surface treatment of the fillers before mixing with the unreacted monomer mixture. Silanes form a bond between the inorganic and organic phases of the RBC. At one end of the molecule, the methoxy functional groups can hydrolyze and interact with the inorganic filler, and at the other end, the methacrylate double bonds can polymerize with the organic monomers. The function of the initiator-accelerator system is to polymerize and cross-link the system into a solid network. The polymerization reaction can be initiated by light activation, self-curing (chemical activation), or dual curing (chemical and light curing) (15).

The most significant changes until recently have been in the reinforcing filler, which has been deliberately decreased in size to produce materials that are easier to polish and more effectively polishable, and that have greater wear resistance. Recent changes have been directed more toward the polymer matrix of the material, primarily the development of systems with controlled polymerization shrinkage and, perhaps more importantly, reduced polymerization shrinkage stress (14).

To reduce the polymerization shrinkage of conventional RBCs, the incremental restorative technique has been used for decades, involving the application of 2 mm thick layers obliquely or horizontally, in an attempt to mitigate stress arising from polymerization shrinkage. The shrinkage stress is highly dependent on the configuration of the cavity. The more walls to which the RBC is bonded during polymerization, the higher the so-called C-factor, which

expresses the ratio of bonded to unbonded surfaces. In the layering technique, a given RBC layer is adapted to one cavity wall, reducing its C-factor and, therefore, its shrinkage stress (17). However, the intricacy of this method demands a significant investment of chair time, and the potential for voids to become trapped between layers remains a concern. Hence, the pursuit of a more streamlined approach led to the development of bulk-fill RBCs (18). Ideally, these are easy-to-handle and forgiving materials. The possibility of bulk filling the cavity has attractive advantages; in particular, the procedure takes less time, and the risk of potential technical errors such as void incorporation and contamination between layers can be reduced (19). These materials possess an extended depth of cure owing to heightened translucency, enabling superior light transmission (20). Moreover, the composition of bulk-fill materials facilitates alterations in the polymerization process by incorporating highly reactive photoinitiators, stress-relieving monomers, and diverse filler variants, including pre-polymer particles and fiberglass rod segments (18).

1.2 Polymerization reaction of RBCs

The radical addition polymerization of dimethacrylate monomers in the RBC consists of three stages: initiation, propagation, and termination.

During the initiation phase, free radicals are released, responsible for starting the polymerization process. Free radicals consist of chemical groups with unpaired electrons and are usually formed by thermal decomposition of molecules, photodissociation, or redox reactions. Photodissociation occurs when a photoinitiator molecule decomposes by absorbing light to form reactive free radicals. This is followed by an exchange of electrons in the initiator-co-initiator system. This process produces free radicals through hydrogen abstraction. The initiator molecule forms a ketyl radical, while the co-initiator molecule becomes an aminoalkyl radical. The remaining electron from the alkene group reaches the opposite end of the monomer, forming a radical monomer. This molecule reacts with a dimethacrylate monomer, creating a chain reaction that ends when two radicals react with each other. The initiation phase is followed by the propagation phase, during which other monomer molecules are rapidly added to the active site, resulting in the growing polymer chain. The propagation reaction continues with an increase in molecular weight and cross-link density until the growing free radical is terminated. Ideally, the propagation reaction can proceed until the supply of monomer molecules is exhausted. However, as the polymer vitrifies due to the increased crosslink density,

the propagation reaction slows down and eventually stops (referred to as autodeceleration), resulting in unreacted dimethacrylates remaining in the RBC restoration. The so-called termination of the reaction can lead to dead polymer chains that are unable to carry out further additions. The polymerized composite resin is extensively cross-linked due to the formation of difunctional carbon double bonds (15, 21).

1.3 Volume changes during polymerization in RBCs

Polymerization usually involves a decrease in volume (shrinkage) as two factors decrease: the Van der Waals volume and the free volume. The Van der Waals volume is the volume of the molecule itself, derived from the atoms and bond lengths. A decrease in Van der Waals volume during polymerization occurs due to changes in bond lengths (conversion of double bonds into single bonds). The free volume of a molecular species, either monomeric or polymeric, is the volume occupied by the molecule as a result of its random rotational and thermal motion. The free volume is reduced when monomers are converted into polymers because the rotation of the polymer chain is more limited than that of an unpolymerized monomer (15, 22). The shifting and spatial organization of monomer molecules cause the volume changes that occur during polymerization. When the polymerization process starts, the resin enters the pre-gel stage, where the organic matrix is in a viscous, plastic form, allowing it to 'flow'. At this stage, monomers can still move into new positions within the organic matrix. The polymerization reaction continues, resulting in the formation of larger molecules, and the RBC becomes hardened and homogenized into a solid body. The stage at which no further displacement is possible is called the gel point and marks the transition from the pre-gel to the post-gel phase. In the post-gel phase, the material is in a rigid, elastic state but is still contracting. This shrinkage causes stress. Gelation is considered the moment when the molecules in the material can no longer compensate for the shrinkage. The complete shrinkage of the material is determined by the stage before gelation, during which the material is still controllable and able to compensate for light curing. The post-gel stage, also called the vitrification stage, is responsible for the formation of residual stresses (23).

1.4 Water absorption

Under clinical conditions, restored teeth are continuously bathed in oral fluids; therefore, water absorption, hygroscopic expansion, and the plasticizing effect can be expected to counteract polymerization contraction and may even compensate for cuspal flexure and neutralize residual shrinkage stresses (24). According to Suiter and colleagues, this stress relaxation takes more than 4 weeks in the case of RBCs. While compensation for polymerization shrinkage is desirable, if hygroscopic expansion exceeds polymerization shrinkage, it can convert the shrinkage stress into an expansion stress, which can be equally damaging (25). Water or solvent absorption into the RBCs can cause swelling, which impacts the dimensions of the restoration. The solvent diffuses into the polymer network and disrupts the chains, causing expansion. However, since the polymer network has porosity and free volume between the chains, particularly near the cross-links, it is theoretically possible for water to be absorbed without a change in volume (26). Additionally, water absorption is associated with the subsequent removal of unreacted components, which would cause a decrease in volume. As such, the dimensional change of a polymer network in the solvent is complex, challenging to predict, and highly material-specific (27, 28). Chutinan et al. have shown that RBC undergoes a volume increase when stored in water, averaging 0.4-1.0% over two months (29). Martin et al. demonstrated a volume increase of 0.5% for RBCs after two years of storage in water (30). For a rigid composite, this expansion can cause stress at the interface with the cavity wall and may even lead to detachment from the cavity. The impact of this increase in volume is significantly mitigated by the fact that the volumetric shrinkage accompanying the polymerization process initially leaves the material 'undersized', and the volumetric expansion resulting from water uptake is usually insufficient to fully compensate for the shrinkage (31). Water uptake may be beneficial in partially compensating for shrinkage, but it compromises the physical properties and biocompatibility of the RBC due to hydrolytic- and biodegradation of the bonds and leaching of unreacted components (32).

1.5 Polymerization stress

The shrinkage leads to the formation of stress not only within the restoration itself and at the restoration-tooth interface but also within the tooth structure (33, 34). The consequences of polymerization stress can lead to a range of clinically relevant issues, including the formation of marginal and internal gaps, microleakage that allows infiltration by saliva and bacteria,

micro-cracking (of the restorative material and/or the tooth itself), marginal staining, and even cuspal movement (35, 36). These factors may jeopardize the long-term success of the restoration. Among these challenges, the presence of internal voids and gaps is particularly undesirable due to their potentially adverse impacts on the chemical and mechanical properties of RBC (37, 38). These voids can serve as sites for crack initiation, while gaps may induce fluid flow within the dentin tubules during activities such as mastication or temperature changes, thereby resulting in post-operative sensitivity (39). The degree of polymerization stress results from several variables, including cavity size (volume factor), cavity configuration (C-factor), RBC composition (including factors such as filler type, size, and filler load, and monomer mixture), the selected restoration technique (incremental or bulk filling), and the light-curing protocol (including the type of the initiator system) (9).

The C-factor generally serves as an effective measure of shrinkage stress, especially in scenarios with similar cavity volumes. As the volume of the cavity increases, an increase in polymerization shrinkage and consequent void formation becomes evident (40). The volume of the cavity not only affects polymerization shrinkage but also reduces the fracture toughness of the tooth, which results from the loss of hard tissue (41). The volumetric shrinkage of RBCs is proportional to their degree of conversion (22, 42).

1.6 Degree of conversion (DC)

The degree of conversion (DC) pertains to the extent of monomer transformation into polymers and is defined as the percentage of reacted C=C bonds in the network. During the polymerization of light-cured RBCs, the monomer conversion is always incomplete (43, 44), leaving residual unsaturation in the form of free or pendant methacrylate groups. This occurs due to the gel effect, which decreases the diffusion rate of the components of the organic mixture and blocks the polymer network, preventing their complete polymerization transformation (45). The DC exhibits a strong correlation with the mechanical characteristics, biocompatibility, and color stability of RBC restorations, and thus, is anticipated to influence clinical outcomes (46). Ensuring satisfactory polymerization in each layer of the RBC is crucial, as inadequate polymerization within the deeper regions of the restoration can contribute to mechanical and physical inadequacies, gap formation, marginal leakage, and potential harm to the pulp, which may ultimately lead to the failure of the RBC restoration (43, 47). The DC is influenced by a

multitude of factors and constitutes a complex interplay, with notable correlations also existing between DC and shrinkage stress (9, 48).

1.7 Fracture toughness

When clinicians select an RBC material, they should keep in mind that although RBCs are somewhat rigid materials, they do not lack strength or stiffness, but rather toughness (49, 50). According to the most modern trends, the rehabilitation of lost tooth structure is based on the biomimetic approach. Biomimetic dentistry seeks to mimic nature by focusing on the tooth's structure, function, and biology as references for the design and implementation of new or improved materials and techniques for the biomechanically optimal restoration or replacement of teeth (51). From a biomimetic perspective, dentists aim to replace lost dental tissue with artificial restorative materials that have similar physical properties to the missing tissues, particularly in terms of flexural strength, flexural modulus, and coefficient of thermal expansion. However, the fracture toughness of particulate-filled RBCs is significantly lower than that of dentin, presenting yet another inherent problem of RBC materials (50, 52). Cohesive fractures within the restoration, adhesive failures at the margins, and secondary caries are cited as the most significant problems associated with the failure of posterior RBCs (53, 54). Fracture toughness is a mechanical property defined as a brittle material's resistance to rapid crack propagation under an applied load. Thus, it is an inherent property of the material that describes its damage tolerance and can be used to anticipate structural performance (49, 50, 53, 54). The issue of lacking fracture toughness is especially apparent in extensive direct RBC restorations, as the volume of the material increases in these cases (40, 54, 55, 56). The fracture toughness values are determined by the physical properties and chemical formulation of the individual components of the restorative material (51). Additionally, particulate-filled RBCs do not have the same microstructure as dentin. A particulate-filled RBC consists of filler particles embedded in a resin matrix, whereas dentin comprises collagen fibers embedded in a hydroxyapatite matrix (54). For this reason, dentin should be considered a fiber-reinforced composite rather than a particulate-filled composite. Improvements could therefore be achieved by using RBCs with a higher resemblance to dentin and possessing high fracture toughness as a substitute for dentin. A material with high fracture toughness is more resistant to crack initiation and propagation. Consequently, fracture toughness and flexural strength become important criteria for the longevity of dental materials (57, 58).

Since the aim is to mimic the structure and physical properties of natural dentin, it is essential to understand its unique characteristics. Ivancik et al. demonstrated that dentin exhibits increasing crack growth resistance with crack extension in all three regions of the dentin (inner, middle, and outer). The fracture toughness of the inner dentin (2.2 MPa $m^{0.5}$) was significantly lower than that of the middle (7.7 MPa $m^{0.5}$) and outer regions (3.4 MPa $m^{0.5}$). The external toughening, consisting mainly of crack bridging, was estimated to increase the fracture energy by an average of 26% across all three regions. These results suggest that restorations extended into deep dentin are much more likely to cause tooth fracture, as the potential for introducing defects is greater and fracture toughness decreases with depth (59).

Until now, RBCs reinforced with millimeter-scale short glass fibers have been the most promising materials, closely resembling dentin in terms of mechanical properties (60, 61, 62, 63). Garoushi et al. reported that their tested short fiber-reinforced composite (SFRC) is significantly different and possesses superior fracture toughness (2.61 MPa $m^{0.5}$), flexural strength (114-124 MPa), and flexural modulus (9.5 GPa) compared to other tested bulk-fill or conventional RBC materials (64). This was consistent with findings by Bijelic-Donova et al., who also examined the correlation between mechanical tests and compressive fatigue limit values of the tested resins (65). The reported results showed that the fracture toughness and fatigue limit values of SFRC were statistically higher than those of conventional RBCs (65, 66).

1.8 Short-fiber reinforced composite (SFRC)

1.8.1 Composition

In 2013, an SFRC (everX Posterior; GC, Tokyo, Japan) was introduced to the market, designed to mimic the stress-absorbing properties of dentin. This SFRC material is intended for use as a bulk base in high-stress-bearing areas for restoring both vital and non-vital teeth (67). It comprises a resin matrix, randomly oriented E-glass fibers, and inorganic particulate fillers. The resin matrix includes bisphenol-A-glycidyl methacrylate (bis-GMA), TEGDMA, and polymethyl methacrylate (PMMA), forming what is known as a semi-interpenetrating polymer network (semi-IPN). This network provides good bonding properties and enhances the toughness of the polymer matrix (68).

An interpenetrating polymer network (IPN) consists of two polymers, each in network form. In semi-IPNs, one or more polymers are cross-linked, while others remain linear or branched, resulting in a multiphase polymer matrix. The semi-IPN forms during the

polymerization of the dimethacrylate monomers with swelled linear polymer poly(methyl methacrylate) (PMMA). The modulus of elasticity of the cross-linked polymer matrix in fiber-reinforced composites (FRCs) is higher than that of semi-IPNs or linear polymer matrix FRCs. However, linear and semi-IPN polymer matrices offer greater toughness compared to FRCs made from cross-linked thermosets. The semi-IPN polymer matrix in FRCs offers advantages over cross-linked dimethacrylate or epoxy-type polymer matrices in terms of handling properties and bonding to resin-luting cements and veneering composites used in dental laboratory-made restorations and root-canal posts (69).

everX Posterior	
Glass fibers	E-glass fibers
Avarage length of fibers	800 μm
Diameter of fibers	17 μm
Particulate fillers	Barium glass
Main monomers in resin matrix	Bis-GMA, TEGDMA, PMMA
% of fibers (w/w)	5-15%
% of particle fillers (w/w)	Barium glass: 60-70% Silicon dioxide: 1-5%
% of resin matrix (w/w)	Bis-GMA: 10-20% TEGDMA: 5-10% PMMA: 5-10%

Table 1. SFRC composition

1.8.2 Mechanical properties of SFRCs

The effectiveness of fiber reinforcement depends on several factors, including the type of resins used, the length, orientation, and diameter of the fibers, the fibers' aspect ratio, their position within the matrix, the adhesion of the fibers to the polymer matrix, and their impregnation into the resin (64, 66, 70). For fibers to effectively reinforce polymers, it is essential that stress be transferred from the polymer matrix to the fibers (70). This can be achieved by ensuring the fibers are at least as long as the critical fiber length and that the aspect ratio, which is the ratio of fiber length to fiber diameter (l/d), is between 30 and 94 (63, 70). This aspect ratio influences the tensile strength and reinforcement efficiency of the fiber-reinforced material (70). The fiber length distribution in everX Posterior ranges from 0.3 to 1.5

mm, falling within the required critical fiber length and aspect ratio range (63, 66). Thus, it is not surprising that the incorporation of short-fiber fillers into the semi-IPN resin matrix enhances fracture toughness (71). Garoushi et al. have demonstrated that millimeter-scale short fiber fillers can halt crack propagation and increase the fracture resistance of SFRC (60). Furthermore, Garoushi et al. evaluated different available SFRC materials, including Alert, EasyCore, Build-It, TI-Core, and everX Posterior, and concluded that all but everX Posterior had fiber lengths below critical thresholds, which explains why this RBC exhibited higher fracture toughness values (71).

Good adhesion between the fiber and the matrix ensures good load transfer between the two components, enabling the load to be transferred to the stronger fiber so that it functions effectively as reinforcement. The fibers prevent the crack from expanding and form interconnecting bridges behind the propagating crack, which dissipate energy as the fibers pull out, leading to a favorable rather than catastrophic failure. This effect may result from the random orientation and the formation of a fiber network, which appears to enhance the material's ability to resist fracture propagation and reduce stress intensity at the crack tip, where the crack tends to propagate unstably. As a consequence, the flexural properties and fracture toughness are increased (63, 66, 70). Conversely, if the adhesion is not strong, and gaps are induced between the fiber and the polymer matrix, these gaps can act as initial fracture sites in the matrix and promote material degradation, highlighting the significance of this bond (70, 71).

Fibers should be well impregnated (embedded) within the polymer matrix to ensure adequate adhesion to the polymer matrix. Good impregnation of fibers with the resin matrix can be achieved using light-curing dimethacrylate monomers or monomer-polymer systems that form a semi-IPN matrix for the FRC. Adequate adhesion of the fibers to the polymer matrix is a crucial requirement for RBC strength. Ideally, the chemical bond between the polymer and the fibers should be covalent. Proper adhesion requires precise impregnation of the fibers within the matrix, and ideally, all fibers should be completely embedded in the polymer matrix. Silane coupling agents have been effectively used to enhance the adhesion between polymers and glass fibers, as well as other dental substrates. The effectiveness of silane coupling agents is based on their ability to form siloxane bridges and hydrogen bonds on the glass surface (72).

1.8.3 Polymerization shrinkage and microleakage of SFRCs

As discussed earlier, polymerization shrinkage represents one of the most significant challenges associated with light-curing RBCs. In the literature, the average volumetric

shrinkage of RBCs is reported to be between 1.5% and 6% (73). Garoushi and colleagues investigated the polymerization shrinkage of various commercially available posterior RBCs, including bulk-fill RBCs and SFRCs, using the strain gauge method. They found that SFRC exhibited the lowest shrinkage strain at 0.17%, attributing this to the presence of short fiber fillers and plasticization of the polymer matrix. The short, randomly oriented fibers in SFRC provide an isotropic reinforcing effect in bulk form. However, this initially isotropic material can become anisotropic in terms of polymerization shrinkage when applied in incremental layers of 1-2 mm thickness, if the fibers align within the plane of application (62, 64). In the same study, Garoushi et al. noted that the properties of anisotropic materials vary based on the orientation of the reinforcing fibers and that shrinkage is not uniform in all directions, since polymerization shrinkage is constrained by the orientation of the fibers (62).

Therefore, during polymerization, the material is unable to shrink along the length of the fibers and maintains its original horizontal dimensions; however, the polymer matrix between the fibers can still experience shrinkage. Related studies on SFRCs, bulk-fill, and conventional RBCs by Tsujimoto et al. (74) and Bocalon et al. (75) have reached a consistent conclusion that the presence of fiber fillers significantly reduces polymerization shrinkage, in the range of 30-72% (76). In another study, Garoushi and colleagues investigated the impact of fiber size on polymerization shrinkage strain, shrinkage stress, and marginal microleakage of restorations (77). They concluded that the presence of short fibers in the RBCs increases resistance to microleakage while significantly reducing shrinkage stress and microleakage compared to restorations made with particulate filled RBC (77).

1.8.4 Depth of cure of SFRCs

For the application of light-curing resin materials in direct restorations, the depth of the cavity must be considered, as light intensity decreases with distance. Several manufacturers have developed posterior "bulk fill" RBCs designed to be applied in cavity thicknesses of up to 4 mm, which feature improved curing, shrinkage, and physical properties (78). The light intensity at a specific depth and for a given irradiation time is crucial for the degree of monomer conversion to polymer (degree of conversion, see before). This property is significantly linked to mechanical properties, biocompatibility, and color stability, and is thus expected to influence the clinical success of restorations (70, 79, 80). Therefore, it is essential to ensure sufficient irradiation reaches the bottom surface of each incremental layer used to build up the restoration. This concept is known as depth of cure, which can be defined as the extent of polymerization throughout the entire mass of the restoration. Inadequate polymerization can lead to detrimental

effects such as decreased strength, voiding, marginal leakage, recurrent caries, increased solubility, adverse pulpal effects, decreased color stability, and ultimately, restoration failure (79, 81).

Miletic and colleagues investigated the cure depth of SFRCs and various commercially available bulk-fill materials by correlating the DC, Vickers hardness (VH), and translucency parameter (TP) (82). They found that SFRC exhibited a significantly higher TP compared to the other bulk-fill materials tested, achieving a cure depth of 5.09 mm. This depth was comparable to that measured by Goracci et al. for SFRC (83).

1.8.5 Possible disadvantages of SFRC

A possible drawback of SFRCs is the high viscosity of the material, which makes application more challenging than with conventional RBCs. Additionally, it is recommended by the GC Corporation that everX Posterior requires a layer of universal RBC as a capping layer. This layer protects the fibers and provides a polishable surface. The increased surface roughness and high translucency may also compromise the restoration's aesthetics, which might be one of the reasons for the capping. Therefore, everX Posterior can only be used as a base material (84, 70, 85).

1.9 Non-destructive methods to investigate the effects of polymerization shrinkage

Transillumination has long been suggested by Magne et al. (86, 87, 88) and Oliveira et al. (89) as a method for crack detection in both direct and indirect restorations. This non-destructive technique allows for the examination of the effects of polymerization shrinkage and has proven to be an effective method for detecting cracks (89). However, so far, Magne and colleagues have only examined the number of enamel cracks one week after the restorative procedure and after fatigue testing. Thus, their findings are more likely a result of the dynamic loading conditions during the accelerated fatigue testing rather than a direct result of the polymerization shrinkage of the restorative material.

A non-invasive approach using micro-computed tomography (micro-CT) has been introduced to investigate RBCs and their impact on tooth structure. This method allows for the quantification of factors such as polymerization shrinkage stress, microleakage, internal adaptation, and gap formation (90). Internal adaptation describes the extent to which an RBC

restoration conforms to the internal architecture of the tooth. Micro-CT scan data can be used to create a 3D model, enabling precise volume calculations. Recognized for its accuracy and reliability, the micro-CT technique is essential for examining the tooth-restoration interface and quantifying voids (35).

1.10 Objectives

Previous studies have demonstrated the outstanding mechanical properties of SFRC materials. However, there are no studies comparing the use of SFRC materials in bulk-fill versus layering techniques to determine if there is any clinically relevant benefit of one over the other. This raises the question of whether the different application methods result in differences in polymerization shrinkage and its subsequent effects. The objective of our investigations was to assess crack formation (study I) associated with different direct restorative procedures in deep class II MOD cavities. Additionally, we aimed to evaluate the internal adaptation, porosity, and degree of conversion (study II) within the aforementioned restorative techniques in these deep MOD cavities.

The null hypotheses were the following:

Study I. Assessment of cracks in the restored teeth

- The first null hypothesis was that the number of cracks generated by the polymerization shrinkage stress right after the restorative procedure would not differ among the investigated direct RBC restorations.
- The second null hypothesis was that there would not be any difference in terms of crack formation 1 week after the restoration within the investigated restorative methods.
- The third null hypothesis assumes that there is no difference between the different restorative methods-in the 1-week crack number.

Study II. Assessment of internal adaptation and the degree of conversion

Maintaining the continuity of our investigations:

- The fourth hypothesis posited that no discernible differences exist in terms of internal adaptation and porosity between SFRC applications using either the bulk or

layered method. Additionally, this hypothesis proposed that SFRC's internal adaptation and porosity are comparable to those of both conventional and bulk-fill RBCs.

- The fifth hypothesis conjectured that no notable distinction exists in the DC when SFRC is utilized through either the bulk or layering approach. Furthermore, this hypothesis asserted that SFRC's degree of conversion is akin to that of conventional and bulk-fill RBCs.

5. Materials and Method

All procedures of the investigations presented were approved by the Regional Ethics Committee for Human Medical and Biological Research (University of Szeged, Hungary, 4029-SZTE, University of Pécs, Hungary) and the studies were designed in accordance with the Declaration of Helsinki.

A total of 200 mandibular third molars extracted for orthodontic reasons were used. The selected caries-free mandibular third molars had the following dimensions: 8–10 mm oro-vestibular diameter, 9–11 mm mesio-distal diameter, and 6–7 mm crown height measured from the cemento-enamel junction. During the entire study period, between the measurements, the teeth were stored in 0.9% saline solution at room temperature.

1.11 Specimen preparation

Class II MOD cavities were prepared in all 200 teeth. The cavities were 5 mm deep and their oral and vestibular walls were 2.5 mm wide each, like in our previous studies (27, 28, 36). The preparation was performed with a round end parallel diamond (881.31.014 FG – Brasseler USA Dental, Savannah, GA) bur initially positioned at the midline of the occlusal surface of the teeth (determined by dividing the distance between the buccal and lingual cusp tips). The thickness of the opposing walls at the cavity base were continuously checked during the preparation with a digital caliper (Mitutoyo Corp., Kawasaki, Japan) and adjusted to have a uniform 2.5 mm thickness at the base of the cavity. The cavity walls were prepared parallel to the axis of the tooth. The depth of the cavity was evaluated with a 15 UNC periodontal probe (Hu-Friedy Mfg. Co., Chicago, USA) measured from the corresponding cusp tip by touching

the cavity wall with full length of the instrument. The cavity was one continuous cavity with the proximal box having exactly the same width (2.5 mm) and depth (5 mm) as the occlusal one. The cavosurface margins were prepared perpendicular to the tooth surface at the end of the preparation.

After cavity preparation, the teeth were screened for enamel cracks with D-Light Pro (GC Europe, Leuven, Belgium) in "detection mode," at ×4.3 magnification. Teeth with enamel cracks were removed from the sample and replaced with ones that remained crack-free after cavity preparation. Finally, 80 crack-free third molars with MOD cavities were included to study I. and were then randomly distributed into four groups of 20. Another 80, crack-free teeth were used for the study II.

1.12 Restorative procedures

All prepared teeth underwent the same adhesive treatment, as follows. A Tofflemire (1101C 0.035, KerrHawe, Bioggio, Switzerland) matrix was applied, and the enamel surrounding the cavity was etched with 37% phosphoric acid for 15 s, then rinsed with water. After drying the cavity, a one-step self-etch adhesive system (G-Premio Bond, GC Europe) was used according to the manufacturer's instructions. The adhesive was light-cured for 60 s with an Optilux 501 quartz- tungsten-halogen light-curing unit (Kerr Corp., Orange, CA, USA). The average power density of the light source, measured with a digital radiometer, was 800 ± 40 mW/cm^2. The class II cavities were first modified to class I using the centripetal technique, building up the proximal walls with conventional RBC (G-aenial Posterior A3, GC Europe). Then, the cavities were restored in either of the following ways in both the Study I. and II.:

Group 1 (n=20): The cavities were restored with SFRC (everX Posterior, GC Europe) in one 4-mm-thick bulk layer, according to the anatomy of the dentin, leaving 1 mm for occlusal covering with conventional RBC. The SFRC was light-cured for 40 s.

Group 2 (n=20): The cavities were restored with SFRC with an oblique layering technique, according to the anatomy of the dentin. The approximately 2-mm-thick layers were placed overall in 4 mm depth, leaving 1 mm for occlusal covering with conventional RBC. The deeper layers were light-cured for 40 s, and the ones on the surface were only for 20 s.

Group 3 (n=20): The cavities were restored with a bulk-fill RBC (SDR Flow+, Dentsply Sirona, NC, USA) in one 4-mm-thick layer, according to the anatomy of the dentin, leaving 1 mm for occlusal covering with conventional RBC. The bulk-fill RBC was light-cured for 40 s.

Group 4 (control group, n=20): The cavities were restored with conventional RBC (G-aenial Posterior A3, GC, Europe) with an oblique layering technique, according to the anatomy of the dentin and enamel. The layers were approximately 2 mm thick. The deeper layers were light-cured for 40 s, and the ones closer to the surface were only for 20 s.
In groups 1, 2, and 3, the occlusal 1 mm was covered with conventional RBC (G-aenial Posterior A3) and light-cured for 20 s.

The study groups, application methods, the investigated materials, and their composition are presented in Table 2**.** The restorations were finished with a fine granular diamond burr (FG 7406-018, Jet Diamonds, Ft. Worth, TX, USA, and FG 249-F012, Horico, Berlin, Germany) and aluminum oxide polishers (OneGloss PS Midi, Shofu Dental GmbH, Ratingen, Germany).

Group	Application method	Material	Manufacturer	Shade	Organic matrix	Filler	Filler loading (vol%/wt%)
Group 1* 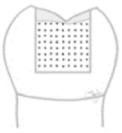	HV SFRC 4mm bulk layer	EverX Posterior	GC Europe, Leuven, Belgium	U	BisGMA, TEGDMA, PMMA	0.7µm barium glass (65.2%), 17µmx1-2mm short E-glass fibers (9%)	53.6/74.2
Group 2* 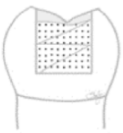	HV SFRC in 2x2mm incremental layers						
Group 3* 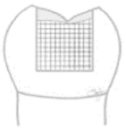	LV bulk-fill RBC in 4mm	Surefil SDR Flow+	Dentsply, Milford, DE, USA	U	Modified UDMA, TEGDMA, DMA, TMA	4.2µm Ba-Al-F-B silicate glass, Sr-Al-F silica, YbF	47.4/70.5
Group 4 (Control) 	HV conventional RBC in 2x2mm incremental layers	G-aenial Posterior	GC Europe, Leuven, Belgium	A3	UDMA, TCDDD, DMA	F-Al-silicate, Sr-glass, lanthanide-F	65.0/77.0

*Table 2. Study groups, materials, application methods, manufacturers, and composition of the investigated resin based composites. * 1mm covering with G-aenial posterior RBC*

The restored teeth were stored in physiological saline solution (Isotonic Saline Solution 0.9%, B. Braun, Melsungen, Germany) in an incubator (mco-18aic, Sanyo, Japan) at 37°C until the start of the experimental procedures.

1.13 Study I. Assessment of cracks in the restored teeth

Screening for cracks was performed with D-Light Pro (GC Europe) at ×4.3 magnification under transillumination with the "detection mode," utilizing a protocol requiring two- examiner agreement (Fig. 1A and B). The light source was used in multiple positions searching for cracks on the external tooth surface for 1–2 minutes in order not to miss any. Only cracks reaching or exceeding the length of 2 mm were considered as shrinkage-induced cracks in our study. The length of the crack was measured with a 15 UNC periodontal probe (Hu-Friedy Mfg. Co., Chicago, USA) positioned parallel to the remaining coronal surface of the tooth next to the crack. The teeth were screened for cracks two times: first after the last polymerization phase and then 1 week later. Between the two sessions, the teeth were kept in physiological saline solution.

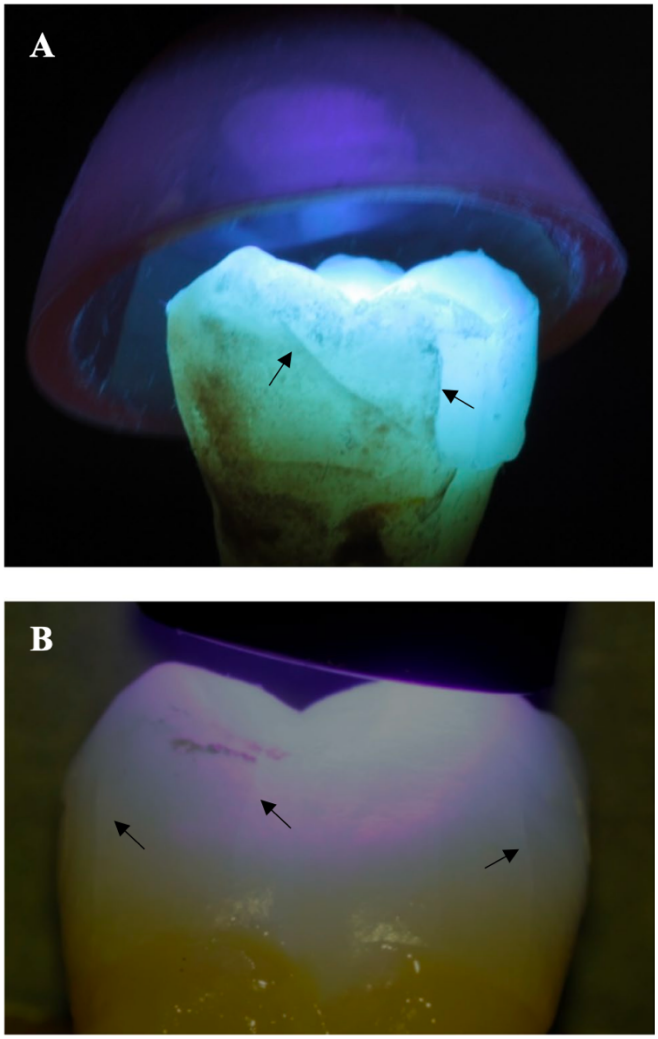

Figure 1. A and B Examples of cracks (arrows) developing during the polymerization process

1.14 Study II. Assessment of internal adaptation and the degree of conversion

1.14.1 Micro-computed tomography measurements – 3D internal adaptation and porosity

To analyze the 3D internal adaptation (IA) and closed pore (CP) volume micro-computed tomography (micro-CT) scans were performed (Skyscan 1176 Control Program: version 1.1 (build 12), Bruker, Kontich, Belgium) of the 80 samples after one month from the polymerization. Each specimen was positioned in a sample holder and scanned for 50 min. After scanning, the samples were stored in dark in an incubator (Cultura, Ivoclar Vivadent, Schaan, Liechtenstein) in 37◦C physiological saline solution. The parameters, such as operating energy (80 kV, 310 µA), resolution (8.74 µm/slice), rotation step (0.7◦), exposure time (1500 ms), and the filter (Al 1 mm) for the micro-CT device were kept constant for all measurements.

Raw image reconstruction and prepare for analysis was performed with SkyScan reconstruction program (NRecon, v.1.7.4.2, Bruker, Kontich, Belgium). The raw images were uniformly reconstructed and multiplanar image sequences were created. Images were converted to 1404 × 1404 pixel resolution in * .bmp format. To evaluate the interfacial gap between the cavity walls and restoration the reconstructed image sequences were rotated to a stan- dardized position so that the plane of the image slices was perpendicular to the vertical axis of the restoration (DataViewer: version 1.5.6.2 64-bit). After the raw image acquisition and reconstruction, the following workflow was applied (Fig. 2 B) of each tooth to analyze the 3D microarchitecture of the images (CT Analyser: version 1.20.8.0 +, Bruker, Kontich, Belgium): identification and designation of region of interest (ROI) at the tooth-restoration interface (including 0.1 mm tooth and 0.1 mm restoration along the interface); binary selection to allow easy separation of the object from the background; image filtering for noise reduction to allow easy recognition of gap at the interface by the software; thresholding, by selecting areas with the same density as air; 3D analysis along the interface of the entire restoration (CTvox: version 3.1.1 r1191, 64-bit) (Fig. 2). The ratio of gap and ROI was calculated and given in percentage. To assess the CP volume, the entire RBC specimen was included to the region of interest (ROI). The pores were calculated using the gray-scale images processed with a Gaussian low-pass filter for noise reduction. A global threshold was used to process the gray level ranges to provide an imposed image of exclusively black and white pixels. The CP volume relative to the total volume of the RBC samples was calculated (%) by measuring the internal voids and specimen volumes of each RBC sample.

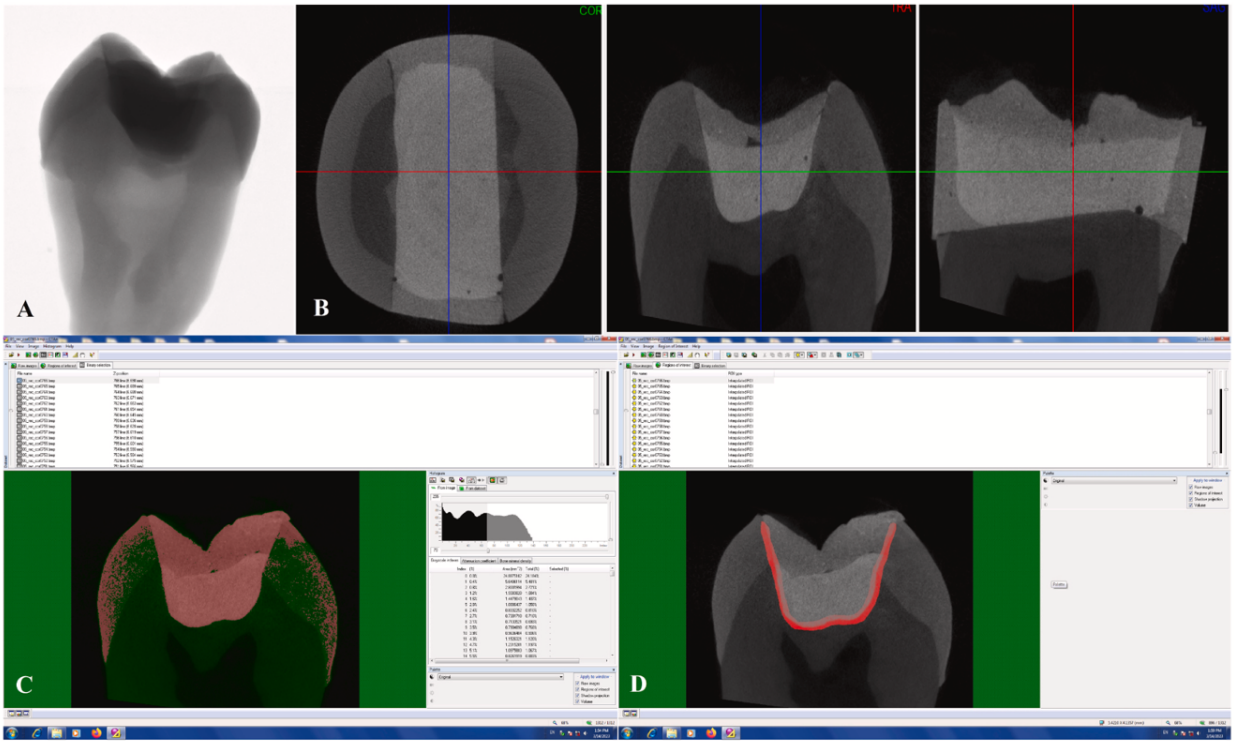

Figure 2. Workflow of 3D internal marginal adaptation analysis: raw image (A), multiplanar image sequences (B), reconstructed image (C), identification and designation of region of interest (ROI) in the axial slices (D)

1.14.2 Scanning electron microscopy – Internal marginal adaptation

After one month storage in physiological saline solution the roots of five restored teeth from each group were removed 2 mm below the cemento-enamel junction and the crowns were cross-sectioned through their centers in a mesio-distal direction, using a water-cooled diamond blade (Isomet Diamond Wafering Blade, no. 11–4244, Buehler Ltd., Lake Buff, IL, USA) (Fig. 3). The halves were polished using a sequence of aluminum-oxide abrasive discs from coarse (50–90 μm) to superfine (1–7 μm) (Sof-Lex Polishing Discs, 3 M, St. Paul, MN, USA) and felt discs (Enamel Plus Shiny FD Interproximal Felt Discs, Micerium, Avegno, Italy) with diamond containing pastes (3 μm - Shiny A and 1 μm - Shiny B, Micerium, Avegno, Italy). The finishing and polishing procedure was performed under constant irrigation with cooled (7 ◦C) physiologic saline. Specimens were cleaned in ultrasonic bath for 10 min to remove debris (Emmi-20HC, eMAG, Salach, Germany). The scanning electron microscopy (SEM) examination of the dentin-restoration interface on the pulpal wall became possible on this vertical section. One half of the teeth were further cross-sectioned horizontally (Fig. 3) and polished with the above described method. Horizontal sectioning provided access to examine the dentin-restoration

interface on the lateral wall. (The other vertical halve was used for Raman measurements.) In order to reduce shrinkage and gap formation due to drying for SEM evaluation, the teeth were immersed in hexamethyldisilazane (HMDS, Millipore Sigma, Burlington, MA, USA) for 10 min, then were left on filter paper in a covered glass vial, and air-dried at room temperature. Thereupon the specimens were sputter-coated with gold to a thickness of 50 nm in a vacuum evaporator (Auto-fine coater, JFC-1300, JEOL, Tokio, Japan) in order to analyze the presence of internal interfacial gaps under scanning electron microscope (SEM) (JEOL JSM-IT500HR, JEOL, Tokio, Japan).

Micrographs were taken from the vertical and horizontal cutting surfaces at standardized magnifications (200X, 400X, 800X), in order to document the bonded internal interface. 2000 µm section of the lateral and the pulpal wall were marked out along the dentin-restoration interface (Fig. 3) to observe and measure the length of the interfacial gaps. The ruler tool of the build in SEM operation control software was used to determine the length of debonded segments along the designated dentin-restoration interface. The SEM image scale bar was used for calibration and the lengths of debonded segments were obtained in micrometers. Data were summed and the total unbonded interface length as a function of the total length of designated section was calculated [(unbonded length/total length) x100 = interfacial gap percentage = IG%].

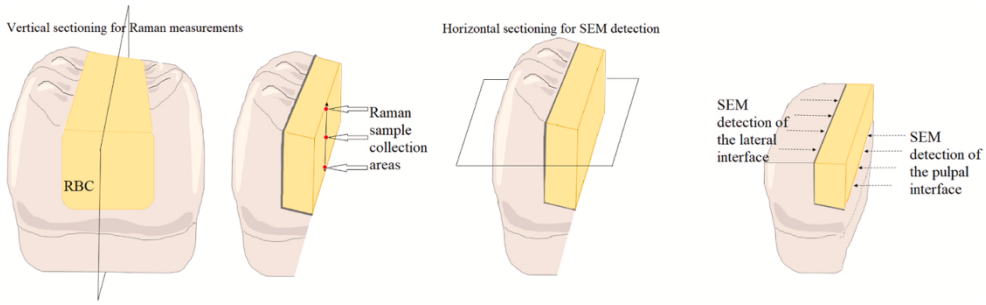

Figure 3. Schematic figure of sample preparation for micro-Raman and scanning electron microscopy (SEM) measurements. The resin-based composite (RBC) fills the cavity which has exactly the same width (2.5mm) and depth (5mm) occluso-proximally. Mesio-distal vertical sectioning provided the sample for the micro-Raman measurements at three different points along the occluso-pulpal diemnsion of the RBC. Horizontal sectioning of the halves provided the sample for SEM measurements along the dentin-restoration interface at a 200 µm section of the lateral and the pulpal wall.

1.14.3 Micro-Raman spectroscopy measurements – degree of conversion

The vertically cross-sectioned teeth (n = 5 per group) (Fig. 3) were mounted on a universal holder that enabled translation along the sample, providing exposure at different depths to the excitation laser light. One-month post-cure DC values were evaluated with a confocal Raman spectrometer (Labram HR 800, HORIBA Jobin Yvon S.A.S., Longjumeau Cedex, France). Raman spectra were collected from three depths of the restoration: 0.5 mm below the surface (top); at the geometric center of the distance between the top and bottom of the sample (middle); and 0.5 mm occlusally from the bottom of the cavity (bottom). During the measurements, the exposed sample surface was about 0.2 mm in diameter with an integration time of 10 s.

The average of ten measurements were collected from three points per each region (top, middle, and bottom). The parameters of the measurements were set according to the following: 20 mW He-Ne laser excitation with 632.817 nm wavelength, magnification x 100 (Olympus UK Ltd., London, UK), spatial resolution ~15 μm, spectral resolution of ~2.5 cm^{-1}. Both diffraction gratings of 600 l/mm and 1800 l/mm are applied. Peltier-cooled CCD (1024 ×256 px) detector is used. Spectra were also taken from the uncured RBCs as reference. Raman data were analyzed between 1440 and 1660 cm^{-1}. The spectra were processed (baseline correction, background correction, and wavelength range se- lection) using LabSpec 5.0 (HORIBA Jobin Yvon S.A.S., Longjumeau Cedex, France) dedicated software for the analysis and post-processing of the spectra. Eight ordered polynomial fit followed by subtraction from the raw data are applied. The Raman vibrational stretching modes at 1458, 1609, and 1640 cm^{-1} were fitted with Lorentzian shapes in order to obtain the absorption peak heights using Origin software package (Origin, Microcal Software Inc., Northampton, MA, USA). DC calculation was performed by comparing the relative change of the band at 1640 cm− 1, representing the aliphatic C– C bonds to a reference band, before and after the polymerization. For EverX Posterior the aromatic C– C band at 1609 cm^{-1} was used as a reference. Due to the lack of the aromatic C– C bonds in the case of G-aenial and SDR, reference band at 1458 cm^{-1} (CH2 deformation) were used (21). DC values were calculated by including the integrated intensities of aliphatic C– C and reference bands in the following formula:

$$DC\% = (1 - (R_{cured}/R_{uncured})) \times 100$$

where R is the ratio of peak intensities at 1640 cm^{-1} and 1609 cm^{-1} or 1458 cm^{-1} (as references) associated to the unconjugated and conjugated carbon bonds or CH2 deformation in non-polymerized and polymerized RBCs, respectively.

1.15 Statistical analysis

For Study I. sample size estimation was done in G*Power 3.1.9.7 (RRID:SCR_013726), with the following input parameters: f=0.35; α=0.05;1-β=0.8; number of groups=4. The required sample size turned out to be n=96, but we chose to start out with 110 specimens, allowing for dropout.

For Study II. the estimated sample size were calculated according to previous study results (91, 92) and with the following sample size formula (93).

Sample size formula:

$$n = \frac{(z1 - \frac{\alpha}{2} + z1 - \beta)^2 (s1 + s2)^2}{(M1 - M2)^2}$$

[z = standard score; α = probability of Type I error at 95% confidence level = 0.05; $z1-\alpha/2$ = 1.96 for 95% confidence; β = probability of Type II error =0.20; 1− β=the power of the test =0.80; $z1-\beta$ =value of standard normal variate corresponding to 0.80 value of power = 0.84; $s1$ = standard deviation of the outcome variable of group 1 = 1.5; $s2$ = standard deviation of the outcome variable of group 2 = 0.8; $M1$ = mean of the outcome variable of group 1 = 67.4; $M2$ = mean of the outcome variable of group 2 = 64.5. For IA determination the $s1$ = 0.12; $s2$ = 0.18; $M1$ = 0.71; $M2$ = 0.42. For DC determination the $s1$ = 1.5; $s2$ = 0.8; $M1$ = 67.4; $M2$ = 64.5. The predicted sample size (n) for IA and DC measurements was found to be a total of 8.4 and 4.9 samples per group, respectively. According to the calculation n = 20 and n = 5 per group sample size was selected for IA/CP and DC measurements, respectively.

The statistical analyses were performed with SPSS (Version 26.0 and 28.0; IBM, Armonk, NY, USA).

For the descriptive characterization of the crack counts in each groups, means (with standard deviations) and medians (with minima and maxima) were calculated. For normality testing, the Shapiro-Wilk test was used. As the distribution of the data was non-normal in most cases, nonparametric tests were chosen for the hypothesis tests. Between-groups comparisons at one given time point were carried out with the Kruskal-Wallis test with post hoc pairwise comparisons, and for the within-group comparisons between the two time points, we used the Wilcoxon matched-pairs test. Where it was necessary because of the multiple comparisons, the level of significance was reduced to $p < 0.0125$.

To analyze data of the DC values, internal gap volume and closed porosity volume Kolmogorov-Smirnov test was applied to test the normal distribution of the data, followed by a parametric statistical test. The DC values, internal gap volume, and closed porosity volume of the samples were compared with one-way analysis of variance (ANOVA). Tukey's post hoc adjustment was used for multiple comparison. Univariate analysis of variance was applied to test the effect of the material (RBC type), filling method (bulk vs. layered) and their interaction on the IA, furthermore the material, depth (top, middle, bottom of the sample), and their interaction on the DC. A Pearson product-moment correlation was run to determine the strength of association between the parameters of interest, such as IA, DC, filling technique (bulk vs. layered), and consistency. P values below 0.05 were considered statistically significant.
Given that we managed to include fewer specimens than required for the 80% power, a post hoc power analysis was also performed with n=80. The power of the study was 72% this way.

6. Results

1.16 Study I. Assessment of cracks in the restored teeth

Regarding the number of cracks right after the restorative procedure, a significantly lower number of polymerization-induced cracks were counted in the fiber-reinforced restorations (groups 1 and 2) than in the control group (layered composite filling, p=0.000 and p=0.000, respectively). Comparing either the non-fiber-reinforced groups (group 3 and the control group) or the SFRC groups (groups 1 and 2), the results did not indicate significant difference (Fig. 4 and Table 3).

As for the comparison between the two timepoints (right after the restorative procedures and 1 week post hoc), a significantly higher number of cracks were counted in all groups after a week (group 1 p=0.000, group 2 p=0.000, group 3 p=0.001, control group p=0.000). However, only the control group (layered composite filling) differed significantly from all the other groups (group 1 p=0.001, group 2 p=0.000, group 3 p=0.003) and there was no significant difference between the other groups **(**Fig. 5 and Table 4).

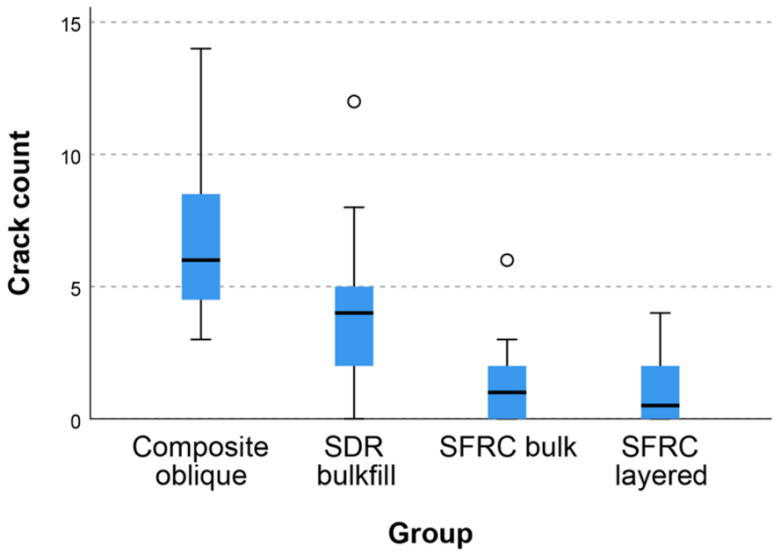

Figure 4. Box plots of the crack counts immediately after restoration

Comparison	Test statistic	Sig. (*p*)
SFRC-layered-SFRC bulk	4.750	1.000
SFRC-layered-SDR bulk-fill	26.125	0.002*
SFRC-layered-composite oblique	43.225	0.000*
SFRC bulk-SDR bulk-fill	21.375	0.020
SFRC bulk-composite oblique	38.475	0.000*
SDR bulk-fill-composite oblique	17.100	.113

Table 3. Pairwise comparisons between the study groups immediately after restoration (Kruskal-Wallis test, post hoc). Asterisk (*) indicates significant difference. The level of significance was adjusted to p=0.0125 according to Bonferroni because of the multiple comparisons

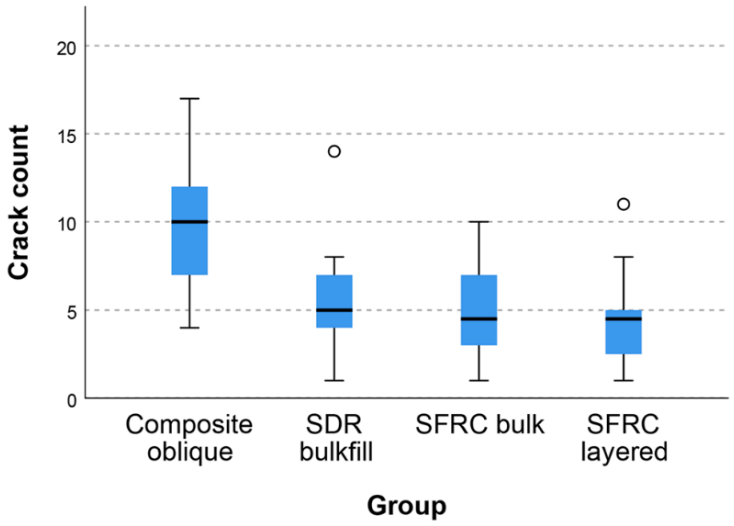

Figure 5. Box plots of the crack counts 1 week after restoration

Comparison	Test statistic	Sig. (*p*)
SFRC-layered-SFRC bulk	4.975	1.000
SFRC-layered-SDR bulk-fill	7.725	1.000
SFRC-layered-composite oblique	33.300	0.000*
SFRC bulk-SDR bulk-fill	2.750	1.000
SFRC bulk-composite oblique	28.325	0.001*
SDR bulk-fill-composite oblique	25.575	0.003*

Table 4. Pairwise comparisons between the study groups 1 week after restoration (Kruskal-Wallis test, post hoc). Asterisk (*) indicates significant difference. The level of significance was adjusted to p=0.0125 according to Bonferroni because of the multiple comparisons.

1.17 Study II. Assessment of internal adaptation and the degree of conversion

1.17.1 Micro-computed tomography measurement - 3D internal adaptation and porosity

The ratio of interfacial gap volume to the total interface volume (ROI for IA) is presented in Fig. 6. The largest gap formation in relation to the examined total interface was detected in the SFRC group filled with layered technique, meanwhile SDR_Bulk revealed the best IA. However, there was no statistically significant difference between the layered

[EverX_Layered vs. G-aenial_Layered: p = 0.124, 95% Confidence Interval (CI): − 0.01–0.11] and the bulk-filled groups (EverX_Bulk vs. SDR_Bulk: p = 0.42, 95% CI: − 0.02–0.09). Regarding the comparison between the bulk-filled vs. layered groups, EverX_Bulk and SDR_Bulk showed statistically significantly lower gap formation compared to EverX_Layered and G-aenial_Layered (EverX_ Layered vs. EverX_Bulk: p < 0.001, 95% CI: 0.15–0.27; G-aenial_Layered vs. EverX_Bulk: p < 0.001, 95% CI: 0.11–0.22; EverX_Layered vs. SDR_Bulk: p < 0.001, 95% CI: 0.19–0.30; G-aenial_Layered vs. SDR_Bulk: p < 0.001, 95% CI: 0.14–0.25). According to the 3D evaluation, the volume of IP relative to the total volume of the RBC sample showed significantly higher values for the layered samples (G-aenial_Layered: 0.15%; EverX_Layered: 0.17%) compared to the bulk RBCs (EverX_Bulk: 0.11%; SDR_Bulk: 0.12%). The one-way ANOVA and the Tukey's post-hoc test revealed significant difference between G-aenial_Layered vs. EverX_Bulk (p = 0.011; 95% CI: 0.01–0.07), and G-aenial_Layered vs. SDR_Bulk (p = 0.045; 95% CI: 0.01–0.07), furthermore, EverX_Layered vs. EverX_Bulk (p<0.001, 95% CI: 0.02–0.09) and EverX_Layered vs. SDR_Bulk (p = 0.002, 95% CI: 0.01–0.08). No significant differences could be detected between the samples made with the layering technique (p= 0.659, 95% CI: -0.05-0.02) or between the bulk groups (p=0.938, 95% CI: -0.04-0.03). Univariate analysis of variance showed a significant effect of the material (RBC type) and filling method regarding the IA [$F(3,76) = 61.6$, $p < 0.001$; $F(1,78) = 166.1$, $p < 0.001$, respectively]. The partial eta-squared was considered to be moderately large ($\eta p2 = 0.71$ and 0.68, respectively). However, their interaction (material x filling method) had an insignificant effect on the gap formation [$F(1,76) = 2.6$, $p = 0.108$; $\eta p2 = 0.03$].

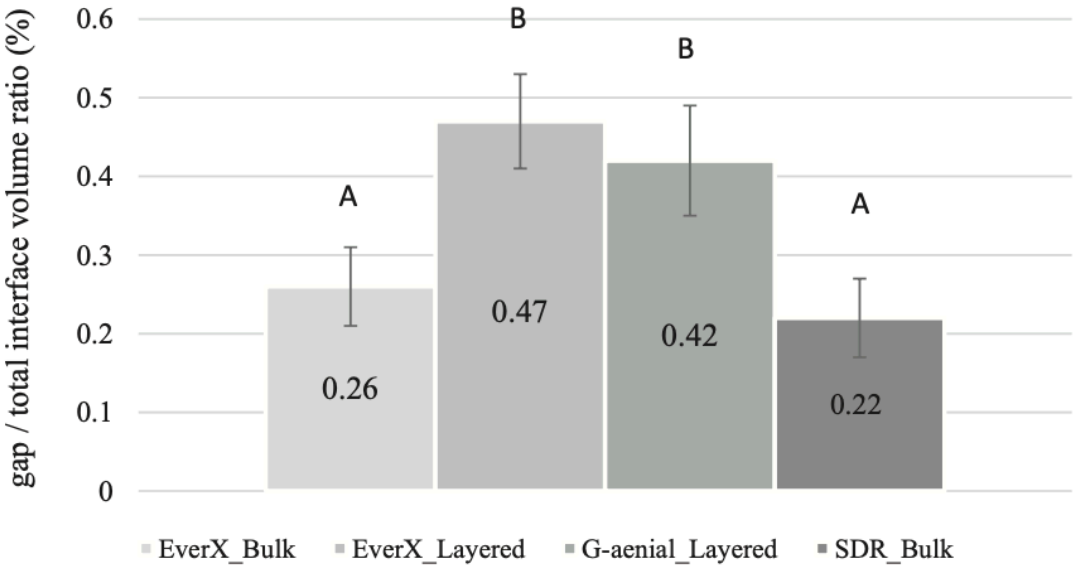

Figure 6. Ratio of interfacial gap volume to the total volume of the designated examined interfacial area (region of interest, ROI) evaluated with 3D micro-computed tomography measurements. Different capital letters indicate a statistically significant difference according to the one-way ANOVA and Tukey's post hoc tests.

1.17.2 Scanning electron microscopy – internal adaptation

Complementary SEM analysis of the pulpal and lateral interfaces of the dentin-RBC revealed comparable performance of the investigated RBC types and application methods on the pulpal floor (Fig. 7A), however, distinct results were visualized on the lateral walls (Fig. 7B).

Figure 8 demonstrates the IG% at the pulpal floor and lateral wall of the examined groups. Interfacial defects at the pulpal interface were detected in similar length (IG% = 100%) for each investigated groups. The interfacial defects mostly developed between the adhesive-RBC interface. Well sealing (IG% = 0%) internal adaptation was demonstrated at the lateral interfaces of SDR_bulk. SEM images of Ever- X_layered demonstrated 70% of IG, meanwhile G-aenial_layered and EverX_bulk groups showed 40% of gap formation along the examined lateral interfacial section. The gaps visible along the lateral walls were formed between the adhesive layer and the dentin.

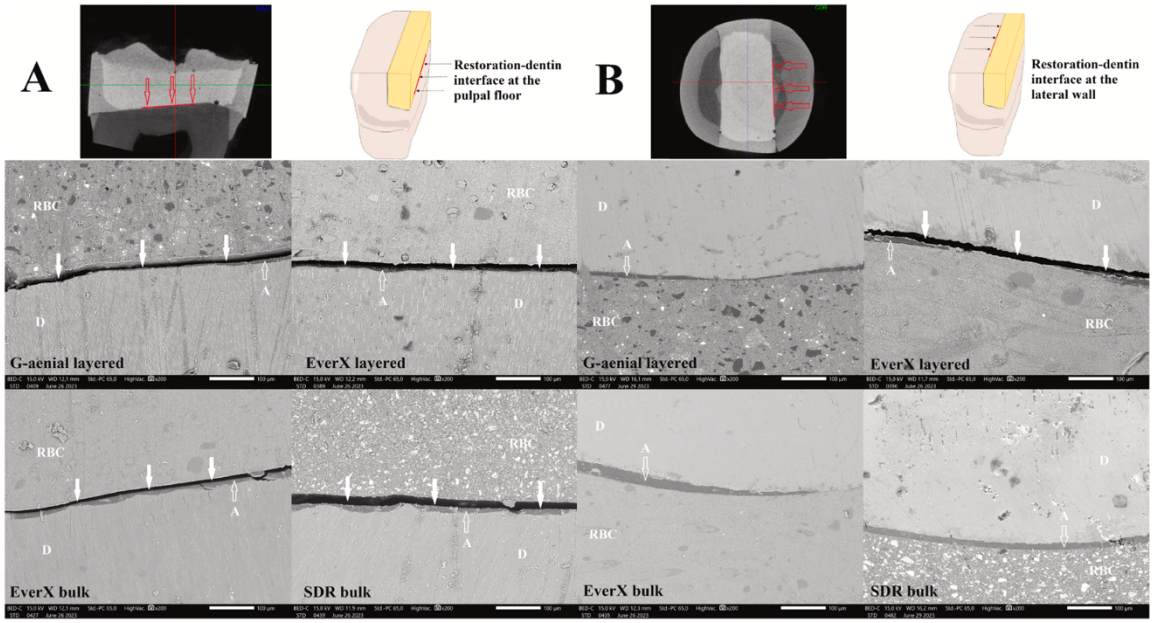

Figure 7. Representative scanning electron microscopy images (200x magnification) of restoration-dentin interfaces at the pulpal floor (A) and lateral wall (B) of the investigated resin-based composites (RBC) applied with layered or bulk technique. Bold white arrows show the interfacial gap; D – dentin, A – adhesive layer.

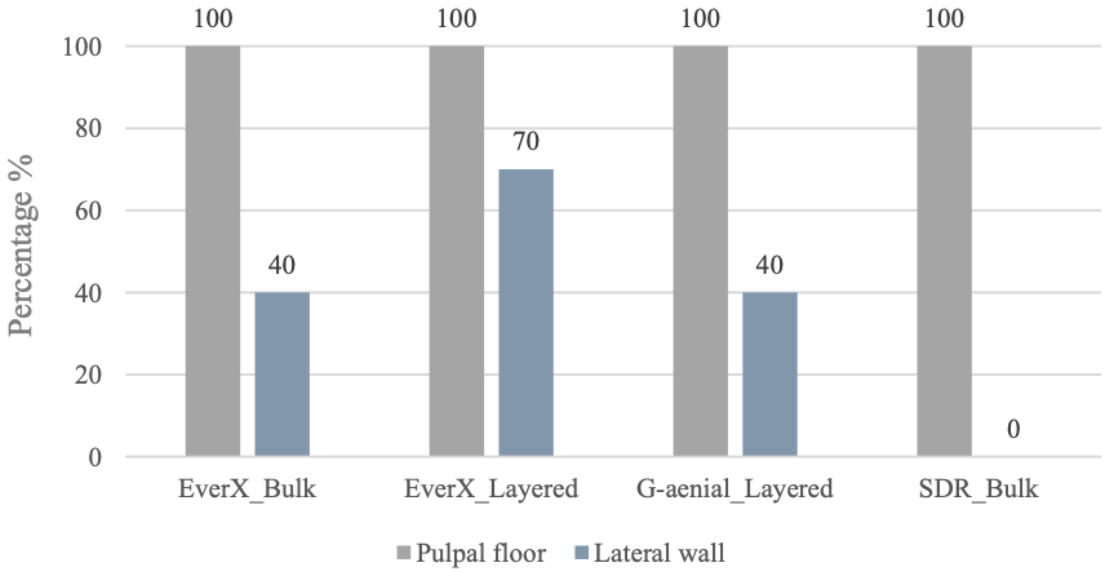

Figure 8. Interfacial gap % (gap/total measured surface) at the pulpal floor and lateral wall of the investigated cavities restored with short-fiber reinforced, conventional and flowable bulk-fill resin-based composites applied in bulk or incremental technique evaluated with scanning electron microscope.

1.17.3 Micro-Raman spectroscopy measurements – degree of conversion

Regarding the DC at the top, middle, and bottom surfaces of the samples, percentages ranged between 77.1–90.7%, 75.9–87.8%, and 74.3–83.2%, respectively. The highest DC values were achieved by G- aenial_Layered group, while EverX_Bulk provided the lowest DC values. When comparing the DC values measured at the top, middle, and bottom of the samples, it was found that both EverX_Bulk and EverX_Layered reached almost the same degree of polymerization throughout the entire depth (Fig. 9). The bottom to top DC ratio (R-DC) of EverX_Bulk and EverX_Layered was 96.4% and 98.7%, respectively. The R-DC of G-aenial_Layered (91.7%) was almost the same as that of SDR_Bulk (91.5%). DC values at the top and bottom showed statistically significant difference in the groups of G-aenial_Layered (95% CI: 1.5–13.4) and SDR_Bulk (95% CI: 2.3–11.7). Furthermore, significant difference was also found between the DC% at the middle and bottom region (95% CI: 0.9–10.3) of SDR_Bulk (Fig. 9).

The comparison of the DC values of the investigated groups by region is presented in Table 5. Statistically significant differences were found among DC% of all groups at the top and middle parts of the samples ($p < 0.05$), except EverX_Bulk and EverX_Layered ($p = 0.961$). At the bottom of the samples, more groups showed similar DC values ($p > 0.05$), except SDR_Bulk vs. G-aenial_Layered ($p = 0.008$), Ever- X_Bulk vs. G-aenial_Layered ($p < 0.001$), and EverX_Layered vs. G- aenial_Layered ($p = 0.008$).

Mixed model ANOVA revealed, that the effect size of material (RBC type) was the highest on the top DC values [$F(3,32) = 25.07$, $p < 0.001$] followed by the DC% at the middle region [$F(3,32) = 18.47$, $p < 0.001$] and then by the DC% at the bottom [$F(3,32) = 8.83$, $p < 0.001$]. The partial eta-squared was considered to be moderately large for each region ($\eta p2 = 0.70$, 0.63, and 0.45, respectively). The analysis of effect size of the depth (top, middle, and bottom region) on the DC values resulted in different findings in the examined groups. The effect size of the depth had a significant impact on DC% of SDR_Bulk [$F(2,24) = 7.66$, $p = 0.003$] and Gaenial_Layered [$F(2,24)2 = 5.04$, $p = 0.015$] with a moderately large partial eta-squared ($\eta p = 0.39$ and 0.30, respectively). The effect of depth on DC% in EverX_Bulk and EverX_Layered seemed to be irrelevant [$F(2,24) = 1.27$, $p = 0.298$, $\eta p2 = 0.09$ and $F(2,24) = 1.13$, $p = 0.339$, $\eta p2 = 0.09$, respectively].

Considering all the investigated groups, the Pearson correlation co- efficient revealed, that the strength of association between IA and DC is small and insignificant [$r(78) = 0.14$, $p = 0.228$], while, the filling technique (bulk vs. layered) has a strong association with IA [$r(78) =$

0.83, $p < 0.001$] and small association with DC [$r(78) = 0.34$, $p = 0.002$]. Since the two bulk groups (EverX_Bulk and SDR_Bulk) had different consistency (EverX was condensable, SDR was flowable), Pearson correlation was run to detect the relation between IA and consistency, furthermore DC and consistency. The results showed strong association between IA and consistency [$r(38)=0.86$, $p<0.001$], while medium between DC and consistency [$r(38) = 0.39$, $p = 0.013$]. Both in IA and DC the flowable consistency contributed to a more favorable outcome.

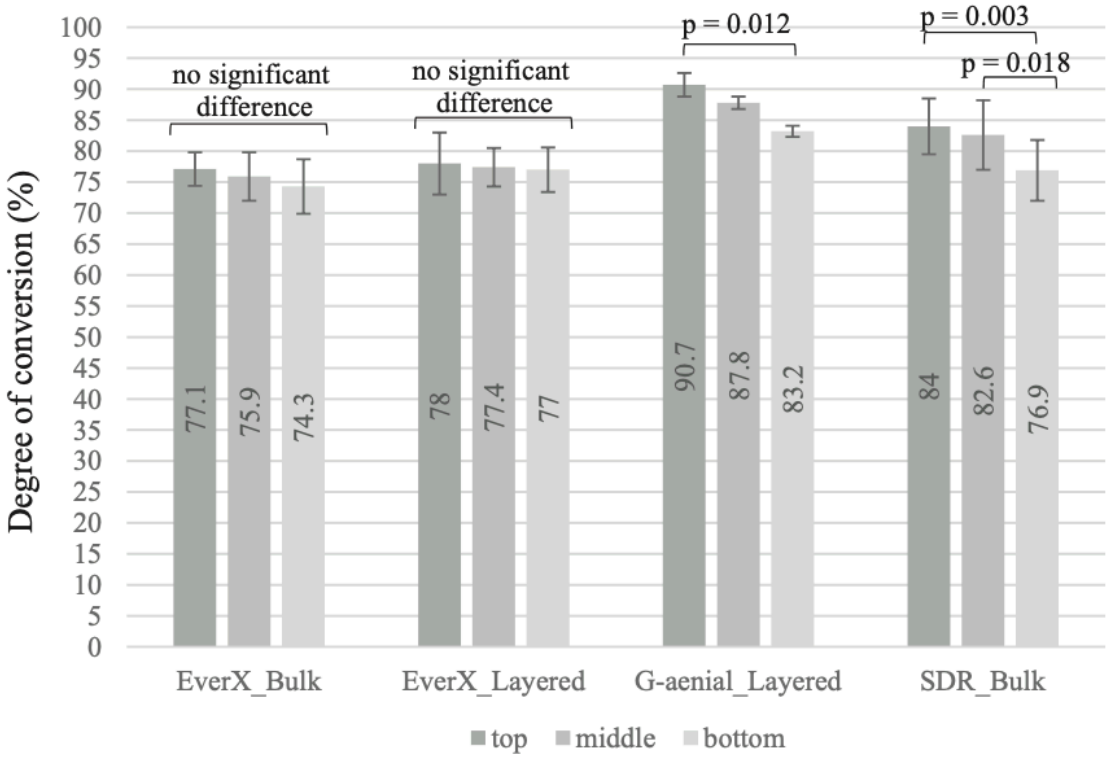

Figure 9. Differences in degree of conversion at the top, middle, and bottom region of the samples within the investigated groups. (Comparison was performed using one-way ANOVA and Tukey's post hoc test).

Region of measurement	Compared groups			Mean DC% difference	95% CI		p-value
					Lower	Upper	
Top	SDR_Bulk	vs.	EverX_Bulk	6.9	2.1	11.7	0003 *
	SDR_Bulk	vs.	EverX_Layered	6.0	1.2	10.8	0,01 *
	SDR_Bulk	vs.	G-aenial_Layered	-6.7	-11.5	-1.9	0004 *
	EverX_Bulk	vs.	EverX_Layered	-0.9	-5.7	3.9	0.961
	EverX_Bulk	vs.	G-aenial_Layered	-13.6	-18.4	-8.8	< 0001 *
	EverX_Layered	vs.	G-aenial_Layered	-12.7	-17.5	-7.9	< 0001 *
Middle	SDR_Bulk	vs.	EverX_Bulk	6.7	1.9	11.5	0004 *
	SDR_Bulk	vs.	EverX_Layered	5.2	0.4	10.0	0031 *
	SDR_Bulk	vs.	G-aenial_Layered	-5.2	-10.0	-0.4	0031 *
	EverX_Bulk	vs.	EverX_Layered	-1.5	-6.3	3.3	0.828
	EverX_Bulk	vs.	G-aenial_Layered	-11.9	-16.7	-7.1	< 0001 *
	EverX_Layered	vs.	G-aenial_Layered	-10.4	-15.2	-5.6	< 0001 *
Bottom	SDR_Bulk	vs.	EverX_Bulk	2.7	-2.2	7.6	0.446
	SDR_Bulk	vs.	EverX_Layered	0.0	-4.9	4.8	1.000
	SDR_Bulk	vs.	G-aenial_Layered	-6.2	-11.1	-1.3	0008 *
	EverX_Bulk	vs.	EverX_Layered	-2.7	-7.6	2.1	0.435
	EverX_Bulk	vs.	G-aenial_Layered	-8.9	-13.8	-4.1	< 0001 *
	EverX_Layered	vs.	G-aenial_Layered	-6.2	-11.1	-1.3	0008 *

*Table 5. Comparison of the degree of conversion (DC%) between the experimental groups on the top, middle, and bottom of the samples (One-way ANOVA and Tukey's post hoc tests, *statistically significant).*

7. Discussion

Despite continuous advancements in the properties of RBCs and adhesives over the past decade (94), achieving optimal integrity and sealing capability for RBCs remains a notable challenge. Inadequate adaptation can give rise to issues like microleakage, secondary caries, discoloration, fracture, and ultimately, restoration loss (95). The effectiveness of tooth-RBC adhesion is influenced by a multitude of factors, including DC, elastic modulus, volumetric polymerization contraction, resulting shrinkage stress, C-factor, curing protocol, and the complex interplay between RBCs, adhesives, and tooth tissues (9, 96).

As already known, polymerization shrinkage stress in RBCs may result in marginal disintegration, cuspal deflection, enamel crack formation, reduced bond strength, compromised mechanical properties, and interfacial gaps between the RBC and the cavity walls, all of which are factors that contribute to the success or failure of direct RBC restorations (36, 97, 98). As a result, polymerization shrinkage-related stress is still deemed a clinically relevant problem in the field of dentistry (9). Cuspal deflection and subsequent enamel crack formation is closely related to cavity dimensions, namely the volume factor (mainly the depth of the cavity) and cavity wall compliance (the continuity and thickness of the remaining walls) (89, 99). As reported by Magne and colleagues, in the posterior region, deep MOD cavities show the highest amount cuspal flexure due to the missing marginal ridges (100). According to Forster et al., in this clinical situation, 5 mm is the critical depth at which material-related disadvantages (such as suboptimal fracture toughness) start to show (41). It is important to note that the number of

direct posterior RBC restorations is expected to increase in such deep cavities with the worldwide phasing out of the use of amalgam (101, 102, 103). Therefore, in our study, we analyzed polymerization shrinkage-induced crack formation of different restorative materials in deep MOD cavities via transillumination.

In the present research, when analyzing crack formation immediately after the restorative procedure, both the bulk-fill and the layered SFRC restorations (groups 1 and 2, respectively) were characterized by significantly fewer cracks compared to layered conventional RBC restorations (control group) ($p=0.000$ and $p=0.000$, respectively) (Fig. 2). Thus, the first null hypothesis was rejected. Until now, SFRC has not been compared to any direct restorative materials in this aspect. The superior results of SFRC might be attributed to its unique structure with short glass fibers of 0.3–1.9 mm embedded in the resin matrix (66).

As the fibers are randomly oriented in the material, they might be able to control the shrinkage and the resulting stress on the cavity walls as the material is not able to shrink in the direction of the fibers, only perpendicular to them (62, 104). Whereas, Fronza et al. showed higher shrinkage stress values of SFRC samples and their result was explained by high inorganic content and resultant high elastic modulus of the material (18). In terms of fracture resistance and failure mode, direct restorations containing SFRC were superior to conventional layered RBC restorations in deep MOD cavities (55, 105). When comparing the layered SFRC group (group 2) with the bulk-fill SFRC group (group 1) regarding crack formation, no difference was found. This is contrary to the findings of Oliveira et al., who found that a significantly higher number of cracks were generated in layered RBC restorations than in bulk-fill RBC fillings (89). However, they tested non-fiber-reinforced RBCs. So far, this is the first study to examine crack formation after restoration with fiber-reinforced and non-fiber-reinforced direct restorative materials applied according to different methods. In our previous studies, we found no difference between layered and bulk-fill direct SFRC restorations in terms of mechanical performance (105, 106). However, crack formation was not evaluated in these studies. Interestingly, only the layered SFRC group (group 2) was superior to the SDR group (group 3) in this respect ($p=0.002$), while there was no difference between the two bulk-fill groups (groups 1 and 3). This is explained in part by the reduced volume of the 2 mm layers compared to the 4 mm bulk increment which may decrease the final polymerization volumetric shrinkage and consequently the shrinkage-induced cracks (14). In contrast, the layering technique did not show this beneficial effect in the control group regarding the crack formation. Boaro et al. demonstrated strong relationship between normalized stress and specimen volume in favor of bulk-fill materials (107); however, Fronza and co-workers refuted this proposition

(18). According to our findings and the above referred conflicting results, it is clear that not only the volume of the material but its composition as well plays an important role in shrinkage stress behaviors. Among the investigated materials, G-aenial Posterior—which served as control—has the highest inorganic filler content of 65 vol% and presented the most cracks, which were developed during and after the polymerization. Although the filler content reduces the volumetric shrinkage, it can increase the material stiffness and thus the elastic modulus (108). Post-polymerization further can increase substantially the Young's modulus (109); however, its opposite in wet storage was also demonstrated (110). Our results support the previous findings, since when comparing the number of cracks right after the restorative procedure and 1 week post hoc, a significant increase was observed in all groups. Thus, the second null hypothesis was rejected. The third null hypothesis, which suggested no significant difference among groups after 1-week water storage, was also rejected, because more prominent differences were observed in the number of cracks at the end of one week. All groups showed significantly fewer cracks compared to the control group (conventional layered RBC restorations). Polymerization process and consequently the shrinkage are known to continue for more than 24 h after light-curing (known as post-cure polymerization) (111). In fact, it has been observed as much as 1 month after photopolymerization (112). As the occurrence of enamel cracks is known to be closely related to the polymerization shrinkage of RBC materials (113), post-cure polymerization should be reflected in the number of cracks after the restorative treatment. The correlation between post-cure polymerization and crack formation is clearly confirmed in our study: the number of cracks significantly increased in all groups during the first week after the restorative procedure (Fig. 4). Interestingly, the effect of hygroscopic expansion could not counterbalance the effect of post-cure polymerization in this respect. Water storage, on the other hand, can plasticize the resin matrix that may also degrade the filler-matrix interface, leading to decrease in Young's modulus and thus in accumulated stress (114). Under clinical conditions, restored teeth are continuously bathed with oral fluids, and thus, water absorption, hygroscopic expansion, and plasticizing effect can be expected to counterbalance polymerization contraction, and thus could even cancel out cuspal flexure and neutralize residual shrinkage stresses (24). According to Suiter and colleagues, this stress-relaxation takes more than 4 weeks in the case of RBC materials (25). Thus, a possible explanation as to why water sorption could not effectively eliminate stress may be that we kept our specimens in water only for a week before the repeated examination. This is in line with the findings of Magne et al. (88). It seems that both SFRC and bulk-fill RBCs are more resilient to polymerization shrinkage-related crack formation than layered conventional high-viscosity RBC fillings.

In addition, another objective of this study was to scrutinize the internal adaptation, porosity, and degree of conversion within SFRC, employed either in bulk or incremental applications. These findings were then juxtaposed with those from a high-viscosity conventional layered RBC and a low-viscosity bulk-fill RBC. To ensure the exclusion of various influencing factors, uniformity was maintained across specimen parameters, encompassing cavity type and size, curing methodology, and adhesive system. The sole variable altered within the experiment pertained to the type of RBC and/or the method of application.

In this ex vivo study, three hypotheses were tested. The first hypothesis assumed that SFRC does not differ in terms of internal adaptation and porosity using the bulk or layering technique, as well as conventional or bulk-fill RBCs. The first hypothesis was partially rejected, as the results of the present study showed that although debonding of the RBCs occurred in all the tested samples, its pattern varied according to the RBC type and application method.
The second hypothesis, which anticipated no difference in the DC if SFRC is used in bulk or layering method, or when compared to conventional or bulk-fill RBCs, was partially rejected. A statistically significant difference was detected in DC among the investigated groups, except for EverX_Bulk vs. EverX_Layered, which showed statistically similar DC values in each investigated region of the restoration (top, middle, and bottom).

The third hypothesis, which assumed that there is no correlation among the parameters of interest, was partially rejected. Strong correlations were detected between IA/filling technique and IA/consistency, as well as a moderate correlation between DC/consistency. Additionally, a small correlation was noted between DC/filling technique. However, the hypothesis regarding the DC/IA relationship should be accepted due to the insignificant association found by the Pearson correlation test.

Utilizing micro-CT technology, we were able to precisely measure the volume of the internal gap and porosity (115). Our findings align with previous research, which similarly concluded that none of the tested materials succeeded in preventing gap formation (116). While gaps were evident across all samples, variations existed in their volume. A more pronounced degree of internal gap (IG) was discernible in groups restored through incremental techniques (EverX_Layered and G-aenial_Layered) when juxtaposed with bulk-filled groups (EverX_Bulk and SDR_Bulk), where a 4-mm increment was employed. Notably, the application of SFRC using both bulk and layered methods revealed greater gap formation, with the layered application exhibiting particularly heightened gap formation. Through Pearson correlation analysis, a robust and significant association between filling technique and internal adaptation was evident. Conversely, Furness et al. reported a contrasting observation, noting

that bulk-fill products exhibited slightly improved outcomes when utilized in an incremental mode compared to being placed within a 4-mm increment (116). To validate the findings derived from the micro-CT measurements, all specimens underwent sectioning and subsequent evaluation through SEM. Concerning the SEM visualization of internal adaptation, a noteworthy correlation emerged between gap volume and the percentage of internal gap (IG%). In congruence with these results, a consistent pattern emerged across all examined groups, revealing gap development at the pulpal floor, specifically between the RBC and the adhesive layer. Our observations align with existing research, which highlights the pulpal floor as the region most susceptible to gap formation (116). This propensity is attributed to the orientation of shrinkage vectors, directed towards the free or unbonded surface, consequently leading to detachment along the pulpal wall (117). Building upon these findings, Han and Park's study also established that in class II RBC restorations, the internal adaptability of the gingival floor within the proximal box and the pulpal floor of the cavity exhibited poorer outcomes compared to the buccal and lingual walls (90). This outcome was explained by the discrepancy between the occluso-gingival height and the bucco-lingual width. As the RBC undergoes polymerization, the shrinkage vector could be more pronounced along the occluso-gingival axis compared to the bucco-lingual axis (90). Diverging perspectives emerge when considering the characteristics of dentinal tubules within a deep cavity floor in contrast to those present in the outer superficial dentin. Notably, the diameters of dentinal tubules vary, consequently impacting the volume of fluid-filled tubule lumens near the pulpo-dentinal junction. Moreover, the peritubular dentin either assumes a thinner composition or is absent altogether (118). SEM images consistently revealed that in all examined groups, separation at the pulpal floor occurred between the adhesive layer and the RBC. This phenomenon finds explanation in the osmosis effect, as elucidated by Van Landuyt et al. (119). According to this theory, the oxygen inhibition layer present at the uppermost region of the adhesive forms a hypertonic zone due to the presence of uncured monomers. In contrast, the dentin, characterized by water-filled tubules and collagen-bound water, represents a hypotonic region. Consequently, water diffusion (osmosis) transpires through the cured adhesive, leading to the emergence of water droplets on the adhesive surface (119). The functional monomers inherent to single-step self-etch adhesives assume the role of semi-permeable membranes due to their robust hydrophilic nature. This attribute contributes to the occurrence of phase separation at the adhesive-RBC interface (120). Under these circumstances, conditions for dentin bonding are suboptimal, rendering the pulpal floor potentially less conducive to dentin bonding when compared to the occlusal sections of the buccal and lingual walls. Variations in the orientation of dentinal tubules further contribute

to these distinctive bonding characteristics across different regions. In agreement with the aforementioned phenomenon, our findings substantiated reduced gap occurrences on the lateral walls, though notable differences emerged among the groups. Within the EverX_Layered group, 70% of the lateral interfaces exhibited gap formation, while the IG% for EverX_Bulk and G-aenial_Layered was 40%, and no gaps were identified on the lateral walls of SDR_Bulk specimens. Although micro-CT volumetric measurements revealed no significant distinctions between the layered and bulk placements, it is plausible that the dissimilarities in IG% as detected by SEM, and the gap volume quantified through micro-CT, stem from variations in the size of interfacial gaps formed. However, contrary to our observations, prior investigations have suggested that the incremental technique yields superior internal adaptation compared to the bulk-fill approach (18, 95), or results in an equivalent proportion of gap-free internal interfaces (116, 121). Across numerous experiments, a robust and positive correlation has been established between internal interfacial gap formation and polymerization shrinkage stress (18, 35, 90). Evaluation of shrinkage vectors has revealed larger mean values in cases of bulk application compared to incremental filling (122). The magnitude of polymerization shrinkage stress is subject to the influence of multiple factors, encompassing filler content, resin system, shrinkage volume, elastic modulus, resin flow, adhesion to the tooth, compliance of cavity walls, and cavity configuration factor (22, 90).

Our disparate outcomes may be partly due to the fact that our measurements were conducted after one-month period of water storage subsequent to polymerization. Post-polymerization, further conversion and subsequent shrinkage/stress could transpire (123). Furthermore, water absorption, associated with resultant swelling and potential hydrolytic degradation, could introduce distinct findings in contrast to immediate post-polymerization assessments (35, 124). Artificial aging has been demonstrated to lead to escalated marginal gap formation and a reduction in the internal adaptation of RBCs (125). However, the absorption of water by RBCs during storage might act as a compensatory mechanism for the effects of initial polymerization shrinkage and shrinkage stress (126). In concurrence with our findings, Park et al. showcased a higher degree of gap expansion for layered RBCs following artificial aging compared to bulk-fill counterparts (125). The infiltration of water into a polymeric structure is subject to the influence of multiple factors, including the degree of conversion (DC) (127), cross-link density (26), and the hydrophilic nature of the network (128). Sorption values have exhibited a noteworthy negative correlation with the extent of filler loading (129). In this study, among the investigated RBCs, G-aenial exhibited the highest filler load, followed by EverX, and subsequently, SDR. This hierarchy of filler content concurs with the observed trends in

internal adaptation (IA). Water sorption, primarily associated with the polymeric phase, is influenced by filler content; as filler content increases, this phenomenon diminishes due to the inverse correlation between filler content and the polymeric matrix (129). An additional explanation may be attributed to the matrix component of RBCs. Elevated levels of triethylene glycol dimethacrylate (TEGDMA) and bisphenol-A glycidyl dimethacrylate (BisGMA) - fundamental constituents of EverX Posterior and SDR - can lead to heightened water absorption, resulting in swelling and plasticization of the RBC (130). However, this rationale fails to elucidate the disparities observed between the bulk and incrementally applied SFRC samples. Kaisarly et al. suggested that clinicians opt for incremental application of bulk-fill RBCs to mitigate stress on the bond, thereby preserving interfacial integrity (122). Our findings concerning SFRC do not support this claim, as EverX Posterior, when applied using the incremental technique, exhibited inferior internal adaptation compared to the bulk technique. A distinguishing feature of EverX lies in its specialized filler load, specifically the inclusion of short E-glass fibers. These fiber-reinforced RBCs have demonstrated greater hygroscopic expansion when contrasted with other fiber-reinforced or particulate-filled RBCs (131). Viewed from a different perspective, the haphazardly oriented glass fibers may possess the capacity to mitigate shrinkage/stress. As polymerization shrinkage along the glass fibers is thought to be constrained, occurring exclusively perpendicular to the fibers, a more advantageous fracture resistance of the restored teeth may result (41, 62). When SFRC is introduced into the cavity via a capsule in a 4 mm bulk quantity, both the resin matrix molecules and the randomly oriented fibers are somewhat aligned in the direction of flow (132). Yet, when employing the incremental technique with SFRC, the layers must be compacted against the cavity walls, potentially inducing a coerced parallel orientation of the fibers. This shift in fiber alignment may alter the trajectory of shrinkage vectors, potentially yielding increased shrinkage perpendicular to the fibers (15). This could contribute to a reduced presence of gap-free interfaces and/or a higher gap volume. An assessment of shrinkage vectors divulged that subsequent increments become well-bonded to the oxygen-inhibited layer of preceding increments, which are drawn upward during layering (133). Additionally, the lower DC of the first increment would apparently maintain greater flexibility in moving upwards (133). Conversely, the heightened translucency of 2 mm SFRC facilitates deeper light penetration during curing, culminating in amplified shrinkage vector values and, consequently, an elevated upward displacement of the first increment (134).

The smallest gap volume, as discerned from the present micro-CT assessment, was observed in the context of the flowable SDR. This particular RBC stands out due to its heightened flexibility

and diminished shrinkage stress, attributes attained through the incorporation of patented modified urethane dimethacrylate and the utilization of a polymerization modulator (122). Several studies have corroborated that this low-viscosity bulk-fill exhibits lower polymerization shrinkage stress compared to other low-viscosity (both conventional and bulk-fill) RBCs, as well as conventional high-viscosity RBCs (135). However, in contrast to these findings, Park et al. (125) reported no disparity in the adaptation of SDR compared to other RBCs.

Regarding location and extent, our results aligned with other RBCs, showcasing comparable gap formation on the pulpal floor with SDR. Nonetheless, SDR was the only material where no internal gap was found on the lateral walls. Furness et al. similarly detected a substantial percentage of gap formation at the pulpal floor for SDR. Notably, their study also unveiled greater detachment along the lateral interface in the case of SDR compared to other investigated bulk-fill or incrementally placed RBCs (116).

The quality of the adhesive interface plays a key role in internal adaptation. If adhesive bonding fails to counteract shrinkage stress, debonding can occur (133). Separation at the interface contributes to heightened shrinkage vectors, offering greater freedom for shrinkage movement (136). To ensure comparability, a uniform one-step self-etch adhesive (G-Premio Bond, GC Europe) was employed in selective etching mode across all groups in this study. The occurrence of gap formation can be attributed to feeble bonding with dentin and/or robust bonding with enamel on the opposing cavity wall (117). Among adhesive systems, one-step self-etch adhesives are recognized for providing comparatively weaker bond strength (137). An additional rationale for our findings may lie in the diminished polymerization shrinkage stress exhibited by bulk-fill RBCs, which could favorably impact internal adaptation, particularly when coupled with underperforming adhesive systems like the one-step self-etch approach (125). In contrast, the incremental technique, due to multiple photopolymerization stages and consequential contraction stress, along with amplified shrinkage vectors, may further compromise the already delicate dentin-RBC bonding. Shrinkage vectors predominantly manifest axial movement contingent upon bonding conditions. In cases of debonded RBCs, axial movement is directed upward toward the curing light, while bonded RBCs experience shrinkage from the free surface towards the cavity wall (138).

Three-dimensional high-resolution micro-computed tomography was also used for the volumetric assessment of closed porosity, leveraging the method's accuracy in quantitatively gauging and visualizing failures such as air bubbles (37). Although air bubbles and voids can potentially infiltrate RBCs during manipulation, it is important to note that submicron pores are inherently present in RBCs as provided by the manufacturer (37). Porosity stands as a parameter

wielding influence over numerous properties of RBCs, thereby making the determination of closed porosity pertinent from both mechanical and chemical standpoints. Voids serve as defects, introducing a discontinuous phase to the RBC matrix, which has the potential to undermine mechanical properties (37). From a chemical vantage, these pores harbour an oxygen-inhibited layer, potentially leading to heightened release of unreacted monomers (139). Moreover, porosity can elevate the water absorption capacity of the RBC, thereby contributing to the previously detailed alterations in internal adaptation during the aging process (38). The presence of voids has been observed to depend on factors such as RBC consistency, thickness, placement technique, and operator proficiency (140). The outcomes of closed porosity measurement in this study unveiled a notably greater pore volume within the layered RBCs when contrasted with samples employing the bulk-fill approach. This observation aligns with certain findings in the literature (141, 142), although it diverges from others (143). Notably, while it has been documented that the utilization of flowable RBCs may lead to an augmented voids volume in restorations (144), our findings diverge from this notion. Specifically, we found no significant distinction between low and high viscosity bulk-fill groups, akin to the study conducted by Nilsen et al. (37).

Micro-Raman spectroscopy was employed to evaluate the degree of polymerization across the upper, middle, and lower surfaces. The polymerization of RBCs is profoundly influenced by various factors encompassing the resin monomer's chemical structure, filler attributes, photoinitiator type and concentration, layer thickness, opacity, and polymerization conditions, among others (46). To ensure comparability, the curing conditions in our study were standardized, affording a basis for comparing different materials in terms of internal adaptation and degree of conversion (DC). Among the investigated groups, G-aenial_Layered exhibited the highest mean DC% (87.2%), trailed by SDR_Bulk (81.2%), EverX_Layered (77.5%), and EverX_Bulk (75.8%). These DC values are notably high and were attained through prolonged exposure time. It is well-documented that a heightened degree of cure can be achieved by elevating energy density, primarily by extending the exposure time (91). While EverX displayed the lowest DC values among the investigated groups, both EverX_Bulk and EverX_Layered demonstrated excellent depth of cure. Notably, no statistically significant differences in DC% were detected across various Raman detection regions (top, middle, and bottom) for these two EverX groups. Comparing the bulk and incremental application of EverX, the disparities in DC values were deemed insignificant between them. However, EverX_Bulk exhibited slightly lower DC% at the middle and bottom regions of the restoration. Our findings are in line with other research that highlights the enhanced light penetration of translucent SFRC, attributed to

its glass fibers, compared to other RBCs, despite increased light scattering and absorption with greater layer thickness (145). Garoushi et al. similarly reported that, akin to EverX Posterior, SDR demonstrated no substantial correlation between DC and layer thickness (145). In our study, although SDR exhibited a notably high mean DC% at a 4 mm thickness, significant differences in DC were observed between the top, middle, and bottom regions. Furthermore, a significant discrepancy in DC between the top and bottom layers was evident for G-aenial when applied in 2mm increments. Pearson correlation analysis highlighted a moderately strong association between DC and the application method. This suggests that layering in 2 mm increments tends to enhance the degree of polymerization compared to the bulk technique.

However, the role of the RBC's composition, the chemical and physical properties of the monomers, filler type and load, and initiator system, among others, is indisputable in the polymerization kinetics, as supported by the moderately large correlation between DC and material (127). While high DC is preferred due to the advantageous resulting mechanical and chemical properties, DC was found to be in clinical contradiction with polymerization shrinkage (146). Conversely, the influence of the curing mode (irradiance, exposure time) on DC, shrinkage strain, and consequently on IA has also been demonstrated (147). By keeping the curing parameters constant, using the same settings (irradiance and exposure time) for each group, we were able to examine the effect of DC on IA. Although the highest IA was observed in relation to the highest DC in the case of G-aenial_Layered, SDR showed a much more favorable adaptation despite having a similarly high DC value. Considering the SFRC RBCs, while there was a slight, but not significant difference in DC between the bulk and layered groups, a remarkable discrepancy was detected in IA. Given the inconsistent results, the correlation analysis revealed an insignificant association between DC and IA. While a thinner RBC layer is more advantageous in terms of conversion (46), it is supposed that the polymerization rate, and consequently the polymerization shrinkage of a 2 mm layer as opposed to a 4 mm thick increment, can lead to higher stress (148). In bulk polymerization, shrinkage stress at the interfaces may be reduced due to the ability of unpolymerized RBC at the bottom to deform and release stress. However, in the incremental layering technique, more stress may arise from the absence of a deep reservoir of uncured RBC from which to relieve polymerization stresses of the upper RBC segment (116). In terms of DC, a bulk-fill RBC can also achieve a high level, attributed to the higher exothermic reaction reported in bulk-fills (48). The heat released during polymerization can facilitate the mobility of reactive species, allowing for increased DC (111). As demonstrated, low viscosity, greater layer thickness, and increased

translucency (such as SDR_Bulk and EverX_Bulk) predispose to a more significant exothermic reaction and a higher degree of polymerization (48).

Despite the careful sample preparation during our investigation, the destructive effects of tooth sectioning - such as thermal load, shear forces, fatigue, vibration, and structural changes among others - required for SEM and micro-Raman evaluation may affect the results, thus the findings of this in vitro restorative study should be interpreted with caution for an in vivo situation. Evaluation of tissues or their interfaces, such as dentin-RBC, can be accomplished only when these have been prepared with minimum to no artifacts. In order to minimize the effects influencing or modifying the results, the samples were stored in physiological saline solution in an incubator at 37 ◦C for one month to allow complete post-polymerization of the RBCs (149), to alleviate the stress due to water sorption (150), and to prevent dehydration of tooth, RBC and their adhesive interface (151). To prevent thermal effect during specimen sectioning and polishing, which may cause structural degradation and influence the DC, constant irrigation was employed (152).

Although the samples being stored in saline for one month, another limitation of this study is the absence of thermo-mechanical loading. This can partially simulate the oral conditions that affect RBC restorations during function. Kim and Park demonstrated that internal adaptation deteriorated due to cyclic loading (35). While a more pronounced deterioration is expected after thermo-mechanical loading, the differences between the examined groups were detectable even after one month of wet storage, as indicated by the results of the present study.

Furthermore, micro-CT imaging, while allowing a detailed display of interfacial adaptation detectable by X-ray, has a limitation of long measurement times that can lead to dehydration of specimens during scanning, resulting in deformation and false positives. This methodological sensitivity is also applicable to SEM examination, however, to reduce the undesirable changes, HMDS drying, as an alternative method was used to dry the samples (153). Although vacuum sputter-coating may result in debonding as an artifact, SEM, as a visualization tool is a common and well-established method for investigating interfacial gap formation (119, 120, 121).

An additional challenge was posed by the delineation of the interface due to the very similar pixel intensity of the tooth, adhesive layer, and RBC on the micro-CT images. Despite these methodological limitations, micro-CT has proven to be a non-destructive and effective tool for quantitatively determining the volume of internal gaps and closed pores in RBC restorations (115, 117, 125).

Another limitation of our study is that samples were not loaded after crack analyzing to see whether the cracks are directly correlated with fracture behavior and whether they propagate in case of the tested materials under loaded condition or not. In future, this aspect should be studied also. Besides, a further shortcoming of the study is that the direction of cracks (horizontal, vertical, or oblique) was not assessed. Furthermore, D-Light Pro using the "detection mode," specifically designed to detect cracks, was utilized in our study. However, the specificity and sensitivity of the device to detect cracks is not known as this device has not been used for such purposes in scientific literature. It is important to highlight that transillumination cannot give information on the depth-wise extension of cracks, which would hold great importance in clinical practice. This could also be a limitation of our study. Despite these known limitations, the current study is a good start point for future research in the field of material-related shrinkage-stress–induced crack formation.

8. Conclusion and new findigs identified based on the results of the research

Within the limitations of this ex vivo study, it can be concluded that:

- Polymerization shrinkage stress induced material- and placement technique–dependent crack formation in tooth, which phenomenon further progressed 1 week after the restoration.
- SFRC was more resistant to shrinkage stress during the restorative procedure; however, after 1 week, besides SFRC, bulk-fill RBC also showed higher resistance to polymerization shrinkage-related crack formation than layered RBC fillings.
- SRFC can decrease the shrinkage stress-induced crack formation in MOD cavities.
- Bulk placement of RBCs exhibited lower interfacial gap volume and achieved satisfactory DC in deep cavities without significant correlation between these parameters.
- The interfacial gap and DC values were predominantly influenced by the RBC type and filling technique.
- The least interfacial detachment occurred in the teeth restored with the flowable bulk-fill RBC (SDR_Bulk). Incremental insertion of SFRC had no advantage over bulk placement in terms of IA and DC.

Further data from various experiments including simulation of clinical conditions, different curing parameters, and applying distinct adhesive systems among others are necessary to investigate the potential clinical benefits of bulk vs. layered SFRCs.

9. Acknowledgments

First and foremost, I am extremely grateful to my supervisors, Dr. habil Edina Lempel and Dr. habil Márk Fráter, for their invaluable advice, help, continuous support and patience over the years.

I would like to thank Dr. Tekla Sáry for her tremendous help in the research. She has always been an inspiration to me and I will always be grateful for her support.

Thanks to Dr. Lili Fanni Szántó for the assistance in the restoration procedures.

Thanks to Dr. Gábor Braunitzer for his help with the statistical calculations.

I would also like to express my gratitude to my family and friends for their encouragement and support every step of the way.

10. References

1. Lynch CD, Opdam NJ, Hickel R, Brunton PA, Gurgan S, Kakaboura A, Shearer AC, Vanherle G, Wilson NH. Academy of Operative Dentistry European Section. Guidance on posterior resin composites: Academy of Operative Dentistry - European Section. J Dent. 2014 Apr;42(4):377-83. doi: 10.1016/j.jdent.2014.01.009. Epub 2014 Jan 22. PMID: 24462699.
2. Heintze SD, Rousson V. Clinical effectiveness of direct class II restorations - a meta-analysis. J Adhes Dent. 2012 Aug;14(5):407-31. doi: 10.3290/j.jad.a28390. PMID: 23082310.
3. Manhart J, Chen H, Hamm G, Hickel R. Buonocore Memorial Lecture. Review of the clinical survival of direct and indirect restorations in posterior teeth of the permanent dentition. Oper Dent. 2004 Sep-Oct;29(5):481-508. PMID: 15470871.
4. Da Rosa Rodolpho PA, Donassollo TA, Cenci MS, Loguércio AD, Moraes RR, Bronkhorst EM, Opdam NJ, Demarco FF. 22-Year clinical evaluation of the performance of two posterior composites with different filler characteristics. Dent Mater. 2011 Oct;27(10):955-63. doi: 10.1016/j.dental.2011.06.001. Epub 2011 Jul 16. PMID: 21762980.
5. Pallesen U, van Dijken JW, Halken J, Hallonsten AL, Höigaard R. Longevity of posterior resin composite restorations in permanent teeth in Public Dental Health Service: a prospective 8 years follow up. J Dent. 2013 Apr;41(4):297-306. doi: 10.1016/j.jdent.2012.11.021. Epub 2012 Dec 7. Erratum in: J Dent. 2013 Nov;41(11):1132-3. PMID: 23228499.
6. Bernardo M, Luis H, Martin MD, Leroux BG, Rue T, Leitão J, DeRouen TA. Survival and reasons for failure of amalgam versus composite posterior restorations placed in a randomized clinical trial. J Am Dent Assoc. 2007 Jun;138(6):775-83. doi: 10.14219/jada.archive.2007.0265. PMID: 17545266.
7. Opdam NJ, Bronkhorst EM, Roeters JM, Loomans BA. Longevity and reasons for failure of sandwich and total-etch posterior composite resin restorations. J Adhes Dent. 2007 Oct;9(5):469-75. PMID: 18297828.
8. Lempel E, Lovász BV, Meszarics R, Jeges S, Tóth Á, Szalma J. Direct resin composite restorations for fractured maxillary teeth and diastema closure: A 7 years retrospective evaluation of survival and influencing factors. Dent Mater. 2017 Apr;33(4):467-476. doi: 10.1016/j.dental.2017.02.001. Epub 2017 Feb 28. PMID: 28256273.

9. Ferracane JL, Hilton TJ. Polymerization stress--is it clinically meaningful? Dent Mater. 2016 Jan;32(1):1-10. doi: 10.1016/j.dental.2015.06.020. Epub 2015 Jul 26. PMID: 26220776.
10. Lempel E, Tóth Á, Fábián T, Krajczár K, Szalma J. Retrospective evaluation of posterior direct composite restorations: 10-year findings. Dent Mater. 2015 Feb;31(2):115-22. doi: 10.1016/j.dental.2014.11.001. Epub 2014 Dec 2. PMID: 25480695.
11. Klapdohr, S., Moszner, N. New Inorganic Components for Dental Filling Composites. Monatshefte für Chemie (2005). 136, 21–45 doi: 10.1007/s00706-004-0254-y
12. Versluis A, Tantbirojn D, Lee MS, Tu LS, DeLong R. Can hygroscopic expansion compensate polymerization shrinkage? Part I. Deformation of restored teeth. Dent Mater. 2011 Feb;27(2):126-33. doi: 10.1016/j.dental.2010.09.007. Epub 2010 Oct 20. PMID: 20970176.
13. Tantbirojn D, Versluis A, Pintado MR, DeLong R, Douglas WH. Tooth deformation patterns in molars after composite restoration. Dent Mater. 2004 Jul;20(6):535-42. doi: 10.1016/j.dental.2003.05.008. PMID: 15134941.
14. Ferracane JL. Resin composite--state of the art. Dent Mater. 2011 Jan;27(1):29-38. doi: 10.1016/j.dental.2010.10.020. Epub 2010 Nov 18. PMID: 21093034.
15. Craig RG, Powers JM, Sakaguchi RL. Craig's Restorative Dental Materials. Mosby Elsevier, St. Louis, USA, 2006.
16. Gajewski VE, Pfeifer CS, Fróes-Salgado NR, Boaro LC, Braga RR. Monomers used in resin composites: degree of conversion, mechanical properties and water sorption/solubility. Braz Dent J. 2012;23(5):508-14. doi: 10.1590/s0103-64402012000500007. PMID: 23306226.
17. Park J, Chang J, Ferracane J, Lee IB. How should composite be layered to reduce shrinkage stress: incremental or bulk filling? Dent Mater. 2008 Nov;24(11):1501-5. doi: 10.1016/j.dental.2008.03.013. Epub 2008 Apr 22. PMID: 18433857.
18. Fronza BM, Rueggeberg FA, Braga RR, Mogilevych B, Soares LE, Martin AA, Ambrosano G, Giannini M. Monomer conversion, microhardness, internal marginal adaptation, and shrinkage stress of bulk-fill resin composites. Dent Mater. 2015 Dec;31(12):1542-51. doi: 10.1016/j.dental.2015.10.001. Epub 2015 Nov 20. PMID: 26608118.
19. Van Ende A, De Munck J, Lise DP, Van Meerbeek B. Bulk-Fill Composites: A Review of the Current Literature. J Adhes Dent. 2017;19(2):95-109. doi: 10.3290/j.jad.a38141. PMID: 28443833.

20. Bucuta S, Ilie N. Light transmittance and micro-mechanical properties of bulk fill vs. conventional resin based composites. Clin Oral Investig. 2014 Nov;18(8):1991-2000. doi: 10.1007/s00784-013-1177-y. Epub 2014 Jan 11. PMID: 24414570.
21. McCabe JF, Walls AWG. Applied Dental Materials. Blackwell Publishing, Oxford, UK, 2008.
22. Braga RR, Ballester RY, Ferracane JL. Factors involved in the development of polymerization shrinkage stress in resin-composites: a systematic review. Dent Mater. 2005 Oct;21(10):962-70. doi: 10.1016/j.dental.2005.04.018. PMID: 16085301.
23. Milosevic, M. Polymerization Mechanics of Dental Composites – Advantages and Disadvantages. Procedia Engineering. 2016. 149. 313-320. doi: 10.1016/j.proeng.2016.06.672.
24. Meriwether LA, Blen BJ, Benson JH, Hatch RH, Tantbirojn D, Versluis A. Shrinkage stress compensation in composite-restored teeth: relaxation or hygroscopic expansion? Dent Mater. 2013 May;29(5):573-9. doi: 10.1016/j.dental.2013.03.006. Epub 2013 Mar 26. PMID: 23537571.
25. Suiter EA, Watson LE, Tantbirojn D, Lou JS, Versluis A. Effective Expansion: Balance between Shrinkage and Hygroscopic Expansion. J Dent Res. 2016 May;95(5):543-9. doi: 10.1177/0022034516633450. Epub 2016 Feb 24. PMID: 26912221.
26. Ferracane JL. Hygroscopic and hydrolytic effects in dental polymer networks. Dent Mater. 2006 Mar;22(3):211-22. doi: 10.1016/j.dental.2005.05.005. Epub 2005 Aug 8. PMID: 16087225.
27. Kalachandra S, Turner DT. Water sorption of polymethacrylate networks: bis-GMA/TEGDM copolymers. J Biomed Mater Res. 1987 Mar;21(3):329-38. doi: 10.1002/jbm.820210306. PMID: 2951387.
28. Hermesch CB, Wall BS, McEntire JF. Dimensional stability of dental restorative materials and cements over four years. Gen Dent. 2003 Nov-Dec;51(6):518-23. PMID: 15055648.
29. Chutinan S, Platt JA, Cochran MA, Moore BK. Volumetric dimensional change of six direct core materials. Dent Mater. 2004 May;20(4):345-51. doi: 10.1016/S0109-5641(03)00127-1. PMID: 15019448.
30. Martin N, Jedynakiewicz N. Measurement of water sorption in dental composites. Biomaterials. 1998 Jan-Feb;19(1-3):77-83. doi: 10.1016/s0142-9612(97)00157-9. PMID: 9678853.

31. Huang C, Kei LH, Wei SH, Cheung GS, Tay FR, Pashley DH. The influence of hygroscopic expansion of resin-based restorative materials on artificial gap reduction. J Adhes Dent. 2002 Spring;4(1):61-71. PMID: 12071630.
32. Wang X, Song S, Chen L, Stafford CM, Sun J. Short-time dental resin biostability and kinetics of enzymatic degradation. Acta Biomater. 2018 Jul 1;74:326-333. doi: 10.1016/j.actbio.2018.05.009. Epub 2018 May 9. PMID: 29751113.
33. Peutzfeldt A, Mühlebach S, Lussi A, Flury S. Marginal Gap Formation in Approximal "Bulk Fill" Resin Composite Restorations After Artificial Ageing. Oper Dent. 2018 Mar/Apr;43(2):180-189. doi: 10.2341/17-068-L. Epub 2017 Nov 17. PMID: 29148914.
34. Néma V, Sáry T, Szántó FL, Szabó B, Braunitzer G, Lassila L, Garoushi S, Lempel E, Fráter M. Crack propensity of different direct restorative procedures in deep MOD cavities. Clin Oral Investig. 2023 May;27(5):2003-2011. doi: 10.1007/s00784-023-04927-1. Epub 2023 Feb 22. PMID: 36814029.
35. Kim HJ, Park SH. Measurement of the internal adaptation of resin composites using micro-CT and its correlation with polymerization shrinkage. Oper Dent. 2014 Mar-Apr;39(2):E57-70. doi: 10.2341/12-378-L. Epub 2013 Oct 10. PMID: 24111809.
36. Soares CJ, Faria-E-Silva AL, Rodrigues MP, Vilela ABF, Pfeifer CS, Tantbirojn D, Versluis A. Polymerization shrinkage stress of composite resins and resin cements - What do we need to know? Braz Oral Res. 2017 Aug 28;31(suppl 1):e62. doi: 10.1590/1807-3107BOR-2017.vol31.0062. PMID: 28902242.
37. Nilsen BW, Mouhat M, Jokstad A. Quantification of porosity in composite resins delivered by injectable syringes using X-ray microtomography. Biomater Investig Dent. 2020 Jul 6;7(1):86-95. doi: 10.1080/26415275.2020.1784013. PMID: 33458692; PMCID: PMC7782768.
38. Balthazard R, Jager S, Dahoun A, Gerdolle D, Engels-Deutsch M, Mortier E. High-resolution tomography study of the porosity of three restorative resin composites. Clin Oral Investig. 2014 Jul;18(6):1613-8. doi: 10.1007/s00784-013-1139-4. Epub 2013 Nov 28. PMID: 24287890.
39. Ratih DN, Palamara JE, Messer HH. Dentinal fluid flow and cuspal displacement in response to resin composite restorative procedures. Dent Mater. 2007 Nov;23(11):1405-11. doi: 10.1016/j.dental.2006.11.029. Epub 2007 Feb 12. PMID: 17296218.
40. Braga RR, Boaro LC, Kuroe T, Azevedo CL, Singer JM. Influence of cavity dimensions and their derivatives (volume and 'C' factor) on shrinkage stress development and

microleakage of composite restorations. Dent Mater. 2006 Sep;22(9):818-23. doi: 10.1016/j.dental.2005.11.010. Epub 2005 Dec 20. PMID: 16368130.

41. Forster A, Braunitzer G, Tóth M, Szabó BP, Fráter M. In Vitro Fracture Resistance of Adhesively Restored Molar Teeth with Different MOD Cavity Dimensions. J Prosthodont. 2019 Jan;28(1):e325-e331. doi: 10.1111/jopr.12777. Epub 2018 Mar 5. PMID: 29508474.
42. Braga RR, Ferracane JL. Contraction stress related to degree of conversion and reaction kinetics. J Dent Res. 2002 Feb;81(2):114-8. PMID: 11827255.
43. Moldovan M, Balazsi R, Soanca A, Roman A, Sarosi C, Prodan D, Vlassa M, Cojocaru I, Saceleanu V, Cristescu I. Evaluation of the Degree of Conversion, Residual Monomers and Mechanical Properties of Some Light-Cured Dental Resin Composites. Materials (Basel). 2019 Jun 30;12(13):2109. doi: 10.3390/ma12132109. PMID: 31262014; PMCID: PMC6651104.
44. Peutzfeldt A. Resin composites in dentistry: the monomer systems. Eur J Oral Sci. 1997 Apr;105(2):97-116. doi: 10.1111/j.1600-0722.1997.tb00188.x. PMID: 9151062.
45. Obici A.C, Sinhoreti M.A.C., Frollini E, Sobrinho, L.C, Consani S. Degree of conversion of Z250 composite determined by Fourier Transform Infrared Spectroscopy: Comparison of techniques, Storage periods and photo-activation methods. *Mat. Res.* 2004, *7*, 605–610. doi: 10.1590/S1516-14392004000400014
46. AlShaafi MM. Factors affecting polymerization of resin-based composites: A literature review. Saudi Dent J. 2017 Apr;29(2):48-58. doi: 10.1016/j.sdentj.2017.01.002. Epub 2017 Mar 7. PMID: 28490843; PMCID: PMC5411902.
47. Lovász BV, Lempel E, Szalma J, Sétáló G Jr, Vecsernyés M, Berta G. Influence of TEGDMA monomer on MMP-2, MMP-8, and MMP-9 production and collagenase activity in pulp cells. Clin Oral Investig. 2021 Apr;25(4):2269-2279. doi: 10.1007/s00784-020-03545-5. Epub 2020 Aug 26. PMID: 32845470; PMCID: PMC7966645.
48. Lempel E, Őri Z, Kincses D, Lovász BV, Kunsági-Máté S, Szalma J. Degree of conversion and in vitro temperature rise of pulp chamber during polymerization of flowable and sculptable conventional, bulk-fill and short-fibre reinforced resin composites. Dent Mater. 2021 Jun;37(6):983-997. doi: 10.1016/j.dental.2021.02.013. Epub 2021 Mar 10. PMID: 33714623.
49. Rudo DN, Karbhari VM. Physical behaviors of fiber reinforcement as applied to tooth stabilization. Dent Clin North Am. 1999 Jan;43(1):7-35, v. PMID: 9929797.

50. Deliperi S, Alleman D, Rudo D. Stress-reduced Direct Composites for the Restoration of Structurally Compromised Teeth: Fiber Design According to the "Wallpapering" Technique. Oper Dent. 2017 May/Jun;42(3):233-243. doi: 10.2341/15-289-T. PMID: 28467261.
51. Magne P, Belser U. *Bonded Porcelain Restorations in the Anterior Dentition : A Biomimetic Approach*. Quintessence Publishing Co Inc.,U.S.; 2002.
52. Manhart J, Kunzelmann KH, Chen HY, Hickel R. Mechanical properties and wear behavior of light-cured packable composite resins. Dent Mater. 2000 Jan;16(1):33-40. doi: 10.1016/s0109-5641(99)00082-2. PMID: 11203521.
53. Demarco FF, Corrêa MB, Cenci MS, Moraes RR, Opdam NJ. Longevity of posterior composite restorations: not only a matter of materials. Dent Mater. 2012 Jan;28(1):87-101. doi: 10.1016/j.dental.2011.09.003. PMID: 22192253.
54. Lassila L, Keulemans F, Säilynoja E, Vallittu PK, Garoushi S. Mechanical properties and fracture behavior of flowable fiber reinforced composite restorations. Dent Mater. 2018 Apr;34(4):598-606. doi: 10.1016/j.dental.2018.01.002. Epub 2018 Jan 20. PMID: 29366493.
55. Sáry T, Garoushi S, Braunitzer G, Alleman D, Volom A, Fráter M. Fracture behaviour of MOD restorations reinforced by various fibre-reinforced techniques - An in vitro study. J Mech Behav Biomed Mater. 2019 Oct;98:348-356. doi: 10.1016/j.jmbbm.2019.07.006. Epub 2019 Jul 9. Erratum in: J Mech Behav Biomed Mater. 2020 Feb;102:103505. PMID: 31302584.
56. Magne P. Composite resins and bonded porcelain: the postamalgam era? J Calif Dent Assoc. 2006 Feb;34(2):135-47. PMID: 16724469.
57. Kim KH, Okuno O. Microfracture behaviour of composite resins containing irregular-shaped fillers. J Oral Rehabil. 2002 Dec;29(12):1153-9. doi: 10.1046/j.1365-2842.2002.00940.x. PMID: 12472851.
58. Ruddell DE, Maloney MM, Thompson JY. Effect of novel filler particles on the mechanical and wear properties of dental composites. Dent Mater. 2002 Jan;18(1):72-80. doi: 10.1016/s0109-5641(01)00022-7. PMID: 11740967.
59. Ivancik J, Arola DD. The importance of microstructural variations on the fracture toughness of human dentin. Biomaterials. 2013 Jan;34(4):864-74. doi: 10.1016/j.biomaterials.2012.10.032. Epub 2012 Nov 3. PMID: 23131531; PMCID: PMC3511669.

60. Garoushi S, Vallittu PK, Lassila LV. Short glass fiber reinforced restorative composite resin with semi-inter penetrating polymer network matrix. Dent Mater. 2007 Nov;23(11):1356-62. doi: 10.1016/j.dental.2006.11.017. Epub 2007 Jan 3. PMID: 17204319.
61. Garoushi S, Tanner J, Vallittu P, Lassila L. Preliminary clinical evaluation of short fiber-reinforced composite resin in posterior teeth: 12-months report. Open Dent J. 2012;6:41-5. doi: 10.2174/1874210601206010041. Epub 2012 Jan 6. PMID: 22408696; PMCID: PMC3282891.
62. Garoushi S, Säilynoja E, Vallittu PK, Lassila L. Physical properties and depth of cure of a new short fiber reinforced composite. Dent Mater. 2013 Aug;29(8):835-41. doi: 10.1016/j.dental.2013.04.016. Epub 2013 May 29. PMID: 23726127.
63. Lassila L, Garoushi S, Vallittu PK, Säilynoja E. Mechanical properties of fiber reinforced restorative composite with two distinguished fiber length distribution. J Mech Behav Biomed Mater. 2016 Jul;60:331-338. doi: 10.1016/j.jmbbm.2016.01.036. Epub 2016 Feb 16. PMID: 26925697.
64. Garoushi S, Gargoum A, Vallittu PK, Lassila L. Short fiber-reinforced composite restorations: A review of the current literature. J Investig Clin Dent. 2018 Aug;9(3):e12330. doi: 10.1111/jicd.12330. Epub 2018 Feb 25. PMID: 29479830.
65. Bijelic-Donova J, Garoushi S, Vallittu PK, Lassila LV. Mechanical properties, fracture resistance, and fatigue limits of short fiber reinforced dental composite resin. J Prosthet Dent. 2016 Jan;115(1):95-102. doi: 10.1016/j.prosdent.2015.07.012. Epub 2015 Oct 14. PMID: 26460170.
66. Bijelic-Donova J, Garoushi S, Lassila LV, Keulemans F, Vallittu PK. Mechanical and structural characterization of discontinuous fiber-reinforced dental resin composite. J Dent. 2016 Sep;52:70-8. doi: 10.1016/j.jdent.2016.07.009. Epub 2016 Jul 20. PMID: 27449703.
67. Özcan M, Vallittu P. *Clinical Guide to Principles of Fiber-Reinforced Composites in Dentistry*. Woodhead Publishing; 2017.
68. Garoushi S, Mangoush E, Vallittu M, Lassila L. Short fiber reinforced composite: a new alternative for direct onlay restorations. Open Dent J. 2013 Dec 30;7:181-5. doi: 10.2174/1874210601307010181. PMID: 24511331; PMCID: PMC3915317.
69. Vallittu, PK. Interpenetrating Polymer Networks (IPNs) in Dental Polymers and Composites. *Journal of Adhesion Science and Technology* 23, no. 7–8 (2009): 961–72. doi:10.1163/156856109X432785.

70. Vallittu PK. High-aspect ratio fillers: fiber-reinforced composites and their anisotropic properties. Dent Mater. 2015 Jan;31(1):1-7. doi: 10.1016/j.dental.2014.07.009. Epub 2014 Jul 31. PMID: 25088348.
71. Garoushi S, Vallittu PK, Lassila L. Mechanical Properties and Wear of Five Commercial Fibre-Reinforced Filling Materials. Chin J Dent Res. 2017;20(3):137-143. doi: 10.3290/j.cjdr.a38768. PMID: 28808697.
72. Garoushi, S. Fiber-Reinforced Composites. In: Miletic, V. (eds) Dental Composite Materials for Direct Restorations. Springer, Cham. (2018) doi: 10.1007/978-3-319-60961-4_9
73. Ferracane JL. Buonocore Lecture. Placing dental composites--a stressful experience. Oper Dent. 2008 May-Jun;33(3):247-57. doi: 10.2341/07-BL2. PMID: 18505214.
74. Tsujimoto A, Barkmeier WW, Takamizawa T, Latta MA, Miyazaki M. Mechanical properties, volumetric shrinkage and depth of cure of short fiber-reinforced resin composite. Dent Mater J. 2016;35(3):418-24. doi: 10.4012/dmj.2015-280. PMID: 27251997.
75. Bocalon AC, Mita D, Natale LC, Pfeifer CS, Braga RR. Polymerization stress of experimental composites containing random short glass fibers. Dent Mater. 2016 Sep;32(9):1079-84. doi: 10.1016/j.dental.2016.06.006. Epub 2016 Jun 29. PMID: 27370995.
76. Bocalon AC, Mita D, Narumyia I, Shouha P, Xavier TA, Braga RR. Replacement of glass particles by multidirectional short glass fibers in experimental composites: Effects on degree of conversion, mechanical properties and polymerization shrinkage. Dent Mater. 2016 Sep;32(9):e204-10. doi: 10.1016/j.dental.2016.06.008. Epub 2016 Jun 29. PMID: 27372238.
77. Garoushi S, Vallittu PK, Watts DC, Lassila LV. Polymerization shrinkage of experimental short glass fiber-reinforced composite with semi-inter penetrating polymer network matrix. Dent Mater. 2008 Feb;24(2):211-5. doi: 10.1016/j.dental.2007.04.001. Epub 2007 May 24. PMID: 17531311.
78. Ilie N, Hickel R. Investigations on a methacrylate-based flowable composite based on the SDR™ technology. Dent Mater. 2011 Apr;27(4):348-55. doi: 10.1016/j.dental.2010.11.014. Epub 2010 Dec 30. PMID: 21194743.
79. Ferracane JL, Greener EH. The effect of resin formulation on the degree of conversion and mechanical properties of dental restorative resins. J Biomed Mater Res. 1986 Jan;20(1):121-31. doi: 10.1002/jbm.820200111. PMID: 3949822.

80. Lobbezoo F, Ahlberg J, Manfredini D, Winocur E. Are bruxism and the bite causally related? J Oral Rehabil. 2012 Jul;39(7):489-501. doi: 10.1111/j.1365-2842.2012.02298.x. Epub 2012 Apr 10. PMID: 22489928.
81. Musanje L, Darvell BW. Curing-light attenuation in filled-resin restorative materials. Dent Mater. 2006 Sep;22(9):804-17. doi: 10.1016/j.dental.2005.11.009. Epub 2005 Dec 20. PMID: 16364419.
82. Miletic V, Pongprueksa P, De Munck J, Brooks NR, Van Meerbeek B. Curing characteristics of flowable and sculptable bulk-fill composites. Clin Oral Investig. 2017 May;21(4):1201-1212. doi: 10.1007/s00784-016-1894-0. Epub 2016 Jul 6. PMID: 27383375.
83. Goracci C, Cadenaro M, Fontanive L, Giangrosso G, Juloski J, Vichi A, Ferrari M. Polymerization efficiency and flexural strength of low-stress restorative composites. Dent Mater. 2014 Jun;30(6):688-94. doi: 10.1016/j.dental.2014.03.006. Epub 2014 Apr 3. PMID: 24703547.
84. Marjanovic J, Veljovic DN, Stasic JN, Savic-Stankovic T, Trifkovic B, Miletic V. Optical properties of composite restorations influenced by dissimilar dentin restoratives. Dent Mater. 2018 May;34(5):737-745. doi: 10.1016/j.dental.2018.01.017. Epub 2018 Feb 3. PMID: 29402537.
85. Magne P, Carvalho MA, Milani T. Shrinkage-induced cuspal deformation and strength of three different short fiber-reinforced composite resins. J Esthet Restor Dent. 2023 Jan;35(1):56-63. doi: 10.1111/jerd.12998. Epub 2023 Jan 11. PMID: 36629028.
86. Batalha-Silva S, de Andrada MA, Maia HP, Magne P. Fatigue resistance and crack propensity of large MOD composite resin restorations: direct versus CAD/CAM inlays. Dent Mater. 2013 Mar;29(3):324-31. doi: 10.1016/j.dental.2012.11.013. Epub 2013 Jan 1. PMID: 23287406.
87. Soares LM, Razaghy M, Magne P. Optimization of large MOD restorations: Composite resin inlays vs. short fiber-reinforced direct restorations. Dent Mater. 2018 Apr;34(4):587-597. doi: 10.1016/j.dental.2018.01.004. Epub 2018 Jan 20. PMID: 29366492.
88. Magne P, Silva S, Andrada Md, Maia H. Fatigue resistance and crack propensity of novel "super-closed" sandwich composite resin restorations in large MOD defects. Int J Esthet Dent. 2016 Spring;11(1):82-97. PMID: 26835525.
89. Oliveira LRS, Braga SSL, Bicalho AA, Ribeiro MTH, Price RB, Soares CJ. Molar cusp deformation evaluated by micro-CT and enamel crack formation to compare

incremental and bulk-filling techniques. J Dent. 2018 Jul;74:71-78. doi: 10.1016/j.jdent.2018.04.015. Epub 2018 Apr 22. PMID: 29689293.

90. Han SH, Park SH. Comparison of Internal Adaptation in Class II Bulk-fill Composite Restorations Using Micro-CT. Oper Dent. 2017 Mar/Apr;42(2):203-214. doi: 10.2341/16-023-L. Epub 2016 Nov 28. PMID: 27892836.
91. Lempel E, Őri Z, Szalma J, Lovász BV, Kiss A, Tóth Á, Kunsági-Máté S. Effect of exposure time and pre-heating on the conversion degree of conventional, bulk-fill, fiber reinforced and polyacid-modified resin composites. Dent Mater. 2019 Feb;35(2):217-228. doi: 10.1016/j.dental.2018.11.017. Epub 2018 Nov 28. PMID: 30503020.
92. Scotti N, Michelotto Tempesta R, Pasqualini D, Baldi A, Vergano EA, Baldissara P, Alovisi M, Comba A. 3D Interfacial Gap and Fracture Resistance of Endodontically Treated Premolars Restored with Fiber-reinforced Composites. J Adhes Dent. 2020;22(2):215-224. doi: 10.3290/j.jad.a44286. PMID: 32322842.
93. Padam S. Sample size for experimental studies. J Clin Prev Card 2012;1:88–93.
94. Opdam NJ, van de Sande FH, Bronkhorst E, Cenci MS, Bottenberg P, Pallesen U, Gaengler P, Lindberg A, Huysmans MC, van Dijken JW. Longevity of posterior composite restorations: a systematic review and meta-analysis. J Dent Res. 2014 Oct;93(10):943-9. doi: 10.1177/0022034514544217. Epub 2014 Jul 21. PMID: 25048250; PMCID: PMC4293707.
95. Abbas G, Fleming GJ, Harrington E, Shortall AC, Burke FJ. Cuspal movement and microleakage in premolar teeth restored with a packable composite cured in bulk or in increments. J Dent. 2003 Aug;31(6):437-44. doi: 10.1016/s0300-5712(02)00121-5. PMID: 12878027.
96. Han SH, Sadr A, Tagami J, Park SH. Internal adaptation of resin composites at two configurations: Influence of polymerization shrinkage and stress. Dent Mater. 2016 Sep;32(9):1085-94. doi: 10.1016/j.dental.2016.06.005. Epub 2016 Jun 30. PMID: 27372237.
97. Rosatto CM, Bicalho AA, Veríssimo C, Bragança GF, Rodrigues MP, Tantbirojn D, Versluis A, Soares CJ. Mechanical properties, shrinkage stress, cuspal strain and fracture resistance of molars restored with bulk-fill composites and incremental filling technique. J Dent. 2015 Dec;43(12):1519-28. doi: 10.1016/j.jdent.2015.09.007. Epub 2015 Oct 9. PMID: 26449641.
98. Sadr A, Bakhtiari B, Hayashi J, Luong MN, Chen YW, Chyz G, Chan D, Tagami J. Effects of fiber reinforcement on adaptation and bond strength of a bulk-fill composite

in deep preparations. Dent Mater. 2020 Apr;36(4):527-534. doi: 10.1016/j.dental.2020.01.007. Epub 2020 Feb 8. PMID: 32044045.

99. van Dijken JW, Pallesen U. Clinical performance of a hybrid resin composite with and without an intermediate layer of flowable resin composite: a 7-year evaluation. Dent Mater. 2011 Feb;27(2):150-6. doi: 10.1016/j.dental.2010.09.010. Epub 2010 Oct 16. PMID: 20952051.

100. Magne P, Oganesyan T. Premolar cuspal flexure as a function of restorative material and occlusal contact location. Quintessence Int. 2009 May;40(5):363-70. PMID: 19582240.

101. Ástvaldsdóttir Á, Dagerhamn J, van Dijken JW, Naimi-Akbar A, Sandborgh-Englund G, Tranæus S, Nilsson M. Longevity of posterior resin composite restorations in adults – A systematic review. J Dent. 2015 Aug;43(8):934-54. doi: 10.1016/j.jdent.2015.05.001. Epub 2015 May 21. PMID: 26003655.

102. Mikulás K, Linninger M, Takács E, Kispélyi IB, Nagy K, Fejérdy P, Hermann P. Paradigmaváltás a fogmegtartó kezelésben: az amalgámkorszak vége [Paradigm shift in conservative dentistry: the end of the amalgam era]. Orv Hetil. 2018 159(42):1700-1709. Hungarian. doi: 10.1556/650.2018. 31215.

103. FDI World Dental Federation. FDI policy statement on dental amalgam and the Minamata Convention on Mercury: adopted by the FDI General Assembly: 13 September 2014, New Delhi, India. Int Dent J. 2014 Dec;64(6):295-6. doi: 10.1111/idj.12151. PMID: 25417784; PMCID: PMC9376425.

104. Miura D, Ishida Y, Shinya A. Polymerization Shrinkage of Short Fiber Reinforced Dental Composite Using a Confocal Laser Analysis. Polymers (Basel). 2021 Sep 13;13(18):3088. doi: 10.3390/polym13183088. PMID: 34577989; PMCID: PMC8468671.

105. Fráter M, Sáry T, Vincze-Bandi E, Volom A, Braunitzer G, Szabó P B, Garoushi S, Forster A. Fracture Behavior of Short Fiber-Reinforced Direct Restorations in Large MOD Cavities. Polymers (Basel). 2021 Jun 23;13(13):2040. doi: 10.3390/polym13132040. PMID: 34201423; PMCID: PMC8271361.

106. Fráter M, Forster A, Keresztúri M, Braunitzer G, Nagy K. In vitro fracture resistance of molar teeth restored with a short fibre-reinforced composite material. J Dent. 2014 Sep;42(9):1143-50. doi: 10.1016/j.jdent.2014.05.004. Epub 2014 May 21. PMID: 24859462.

107. Boaro LC, Meira JB, Ballester RY, Braga RR. Influence of specimen dimensions and their derivatives (C-factor and volume) on polymerization stress determined in a high compliance testing system. Dent Mater. 2013 Oct;29(10):1034-9. doi: 10.1016/j.dental.2013.07.011. Epub 2013 Aug 9. PMID: 23932210.

108. Masouras K, Silikas N, Watts DC. Correlation of filler content and elastic properties of resin-composites. Dent Mater. 2008 Jul;24(7):932-9. doi: 10.1016/j.dental.2007.11.007. Epub 2007 Dec 21. PMID: 18155132.

109. Braem M, Lambrechts P, Van Doren V, Vanherle G. The impact of composite structure on its elastic response. J Dent Res. 1986 May;65(5):648-53. doi: 10.1177/00220345860650050301. PMID: 3457818.

110. Abe Y, Lambrechts P, Inoue S, Braem MJ, Takeuchi M, Vanherle G, Van Meerbeek B. Dynamic elastic modulus of 'packable' composites. Dent Mater. 2001 Nov;17(6):520-5. doi: 10.1016/s0109-5641(01)00012-4. PMID: 11567690.

111. Par M, Gamulin O, Marovic D, Klaric E, Tarle Z. Effect of temperature on post-cure polymerization of bulk-fill composites. J Dent. 2014 Oct;42(10):1255-60. doi: 10.1016/j.jdent.2014.08.004. Epub 2014 Aug 15. PMID: 25132366.

112. Schneider LF, Consani S, Ogliari F, Correr AB, Sobrinho LC, Sinhoreti MA. Effect of time and polymerization cycle on the degree of conversion of a resin composite. Oper Dent. 2006 Jul-Aug;31(4):489-95. doi: 10.2341/05-81. PMID: 16924990.

113. Han L, Okamoto A, Fukushima M, Okiji T. Enamel micro-cracks produced around restorations with flowable composites. Dent Mater J. 2005 Mar;24(1):83-91. doi: 10.4012/dmj.24.83. PMID: 15881213.

114. Chung SM, Yap AU, Koh WK, Tsai KT, Lim CT. Measurement of Poisson's ratio of dental composite restorative materials. Biomaterials. 2004 Jun;25(13):2455-60. doi: 10.1016/j.biomaterials.2003.09.029. PMID: 14751729.

115. Han SH, Sadr A, Tagami J, Park SH. Non-destructive evaluation of an internal adaptation of resin composite restoration with swept-source optical coherence tomography and micro-CT. Dent Mater. 2016 Jan;32(1):e1-7. doi: 10.1016/j.dental.2015.10.009. Epub 2015 Nov 21. PMID: 26614427.

116. Furness A, Tadros MY, Looney SW, Rueggeberg FA. Effect of bulk/incremental fill on internal gap formation of bulk-fill composites. J Dent. 2014 Apr;42(4):439-49. doi: 10.1016/j.jdent.2014.01.005. Epub 2014 Jan 27. PMID: 24480086.

117. Chiang YC, Rösch P, Dabanoglu A, Lin CP, Hickel R, Kunzelmann KH. Polymerization composite shrinkage evaluation with 3D deformation analysis from microCT images. Dent Mater. 2010 Mar;26(3):223-31. doi: 10.1016/j.dental.2009.09.013. Epub 2009 Nov 13. PMID: 19913900.

118. Pashley DH, Pashley EL, Carvalho RM, Tay FR. The effects of dentin permeability on restorative dentistry. Dent Clin North Am. 2002 Apr;46(2):211-45, v-vi. doi: 10.1016/s0011-8532(01)00009-x. PMID: 12014033.

119. Van Landuyt KL, Snauwaert J, De Munck J, Coutinho E, Poitevin A, Yoshida Y, Suzuki K, Lambrechts P, Van Meerbeek B. Origin of interfacial droplets with one-step adhesives. J Dent Res. 2007 Aug;86(8):739-44. doi: 10.1177/154405910708600810. PMID: 17652202.

120. Tay FR, Pashley DH, Suh B, Carvalho R, Miller M. Single-step, self-etch adhesives behave as permeable membranes after polymerization. Part I. Bond strength and morphologic evidence. Am J Dent. 2004 Aug;17(4):271-8. PMID: 15478490.

121. Heintze SD, Monreal D, Peschke A. Marginal Quality of Class II Composite Restorations Placed in Bulk Compared to an Incremental Technique: Evaluation with SEM and Stereomicroscope. J Adhes Dent. 2015 Apr;17(2):147-54. doi: 10.3290/j.jad.a33973. PMID: 25893223.

122. Kaisarly D, El Gezawi M, Keßler A, Rösch P, Kunzelmann KH. Shrinkage vectors in flowable bulk-fill and conventional composites: bulk versus incremental application. Clin Oral Investig. 2021 Mar;25(3):1127-1139. doi: 10.1007/s00784-020-03412-3. Epub 2020 Jul 11. PMID: 32653992; PMCID: PMC7878238.

123. Halvorson RH, Erickson RL, Davidson CL. Energy dependent polymerization of resin-based composite. Dent Mater. 2002 Sep;18(6):463-9. doi: 10.1016/s0109-5641(01)00069-0. PMID: 12098575.

124. Szczesio-Wlodarczyk A, Sokolowski J, Kleczewska J, Bociong K. Ageing of Dental Composites Based on Methacrylate Resins-A Critical Review of the Causes and Method of Assessment. Polymers (Basel). 2020 Apr 10;12(4):882. doi: 10.3390/polym12040882. PMID: 32290337; PMCID: PMC7240588.

125. Park KJ, Pfeffer M, Näke T, Schneider H, Ziebolz D, Haak R. Evaluation of low-viscosity bulk-fill composites regarding marginal and internal adaptation. Odontology. 2021 Jan;109(1):139-148. doi: 10.1007/s10266-020-00531-x. Epub 2020 Jun 9. Erratum in: Odontology. 2022 Apr;110(2):417. PMID: 32519114; PMCID: PMC8526473.

126. Rosales-Leal JI, Castillo-Salmerón RD, Molino-Serrano MA, González-Moreira H, Cabrerizo-Vílchez MA. Effect of hygroscopic expansion of resin filling on interfacial gap and sealing: a confocal microscopy study. J Adhes Dent. 2013 Oct;15(5):423-30. doi: 10.3290/j.jad.a29529. PMID: 23560254.

127. Gajewski VE, Pfeifer CS, Fróes-Salgado NR, Boaro LC, Braga RR. Monomers used in resin composites: degree of conversion, mechanical properties and water sorption/solubility. Braz Dent J. 2012;23(5):508-14. doi: 10.1590/s0103-64402012000500007. PMID: 23306226.

128. Ito S, Hashimoto M, Wadgaonkar B, Svizero N, Carvalho RM, Yiu C, Rueggeberg FA, Foulger S, Saito T, Nishitani Y, Yoshiyama M, Tay FR, Pashley DH. Effects of resin hydrophilicity on water sorption and changes in modulus of elasticity. Biomaterials. 2005 Nov;26(33):6449-59. doi: 10.1016/j.biomaterials.2005.04.052. PMID: 15949841.

129. Alshali RZ, Salim NA, Satterthwaite JD, Silikas N. Long-term sorption and solubility of bulk-fill and conventional resin-composites in water and artificial saliva. J Dent. 2015 Dec;43(12):1511-8. doi: 10.1016/j.jdent.2015.10.001. Epub 2015 Oct 9. PMID: 26455541.

130. Sideridou ID, Karabela MM, Bikiaris DN. Aging studies of light cured dimethacrylate-based dental resins and a resin composite in water or ethanol/water. Dent Mater. 2007 Sep;23(9):1142-9. doi: 10.1016/j.dental.2006.06.049. Epub 2006 Nov 21. PMID: 17118438.

131. Alshabib A, Algamaiah H, Silikas N, Watts DC. Material behavior of resin composites with and without fibers after extended water storage. Dent Mater J. 2021 May 29;40(3):557-565. doi: 10.4012/dmj.2020-028. Epub 2021 Mar 18. PMID: 33731541.

132. Oumer AN, Mamat O. A study of fiber orientation in short fiber-reinforced composites with simultaneous mold filling and phase change effects. Comp Part B: Eng 2012;43:1087–94.

133. Kaisarly D, El Gezawi M, Xu X, Rösch P, Kunzelmann KH. Shrinkage vectors of a flowable composite in artificial cavity models with different boundary conditions: Ceramic and Teflon. J Mech Behav Biomed Mater. 2018 Jan;77:414-421. doi: 10.1016/j.jmbbm.2017.10.004. Epub 2017 Oct 3. PMID: 29020664.

134. Ilie N, Keßler A, Durner J. Influence of various irradiation processes on the mechanical properties and polymerisation kinetics of bulk-fill resin based composites.

J Dent. 2013 Aug;41(8):695-702. doi: 10.1016/j.jdent.2013.05.008. Epub 2013 May 21. PMID: 23707645.

135. Rizzante FAP, Mondelli RFL, Furuse AY, Borges AFS, Mendonça G, Ishikiriama SK. Shrinkage stress and elastic modulus assessment of bulk-fill composites. J Appl Oral Sci. 2019 Jan 7;27:e20180132. doi: 10.1590/1678-7757-2018-0132. PMID: 30624465; PMCID: PMC6322642.

136. Kaisarly D, El Gezawi M, Lai G, Jin J, Rösch P, Kunzelmann KH. Effects of occlusal cavity configuration on 3D shrinkage vectors in a flowable composite. Clin Oral Investig. 2018 Jun;22(5):2047-2056. doi: 10.1007/s00784-017-2304-y. Epub 2017 Dec 16. PMID: 29248963.

137. El Gedaily M, Attin T, Wiedemeier DB, Tauböck TT. Impact of Different Etching Strategies on Margin Integrity of Conservative Composite Restorations in Demineralized Enamel. Materials (Basel). 2020 Oct 11;13(20):4500. doi: 10.3390/ma13204500. PMID: 33050594; PMCID: PMC7600983.

138. Van Ende A, Van de Casteele E, Depypere M, De Munck J, Li X, Maes F, Wevers M, Van Meerbeek B. 3D volumetric displacement and strain analysis of composite polymerization. Dent Mater. 2015 Apr;31(4):453-61. doi: 10.1016/j.dental.2015.01.018. Epub 2015 Feb 19. PMID: 25702975.

139. Gauthier MA, Stangel I, Ellis TH, Zhu XX. Oxygen inhibition in dental resins. J Dent Res. 2005 Aug;84(8):725-9. doi: 10.1177/154405910508400808. PMID: 16040730.

140. Samet N, Kwon KR, Good P, Weber HP. Voids and interlayer gaps in Class 1 posterior composite restorations: a comparison between a microlayer and a 2-layer technique. Quintessence Int. 2006 Nov-Dec;37(10):803-9. PMID: 17078279.

141. Soares CJ, Rosatto C, Carvalho VF, Bicalho AA, Henriques J, Faria-E-Silva AL. Radiopacity and Porosity of Bulk-fill and Conventional Composite Posterior Restorations-Digital X-ray Analysis. Oper Dent. 2017 Nov/Dec;42(6):616-625. doi: 10.2341/16-146-L. Epub 2017 Oct 4. PMID: 28976845.

142. Dunavári E, Berta G, Kiss T, Szalma J, Fráter M, Böddi K, Lempel E. Effect of Pre-Heating on the Monomer Elution and Porosity of Conventional and Bulk-Fill Resin-Based Dental Composites. Int J Mol Sci. 2022 Dec 19;23(24):16188. doi: 10.3390/ijms232416188. PMID: 36555828; PMCID: PMC9782750.

143. Soto-Montero J, Giannini M, Sebold M, de Castro EF, Abreu JLB, Hirata R, Dias CTS, Price RBT. Comparison of the operative time and presence of voids of

incremental and bulk-filling techniques on Class II composite restorations. Quintessence Int. 2022 Feb 1;53(3):200-208. doi: 10.3290/j.qi.b2218737. PMID: 34709774.

144. Pardo Díaz CA, Shimokawa C, Sampaio CS, Freitas AZ, Turbino ML. Characterization and Comparative Analysis of Voids in Class II Composite Resin Restorations by Optical Coherence Tomography. Oper Dent. 2020 Jan/Feb;45(1):71-79. doi: 10.2341/18-290-L. Epub 2019 Jun 21. PMID: 31226004.

145. Garoushi S, Vallittu P, Shinya A, Lassila L. Influence of increment thickness on light transmission, degree of conversion and micro hardness of bulk fill composites. Odontology. 2016 Sep;104(3):291-7. doi: 10.1007/s10266-015-0227-0. Epub 2015 Dec 11. PMID: 26660101.

146. Amirouche-Korichi A, Mouzali M, Watts DC. Effects of monomer ratios and highly radiopaque fillers on degree of conversion and shrinkage-strain of dental resin composites. Dent Mater. 2009 Nov;25(11):1411-8. doi: 10.1016/j.dental.2009.06.009. Epub 2009 Aug 15. PMID: 19683808.

147. Silikas N, Eliades G, Watts DC. Light intensity effects on resin-composite degree of conversion and shrinkage strain. Dent Mater. 2000 Jul;16(4):292-6. doi: 10.1016/s0109-5641(00)00020-8. PMID: 10831785.

148. Xu T, Li X, Wang H, Zheng G, Yu G, Wang H, Zhu S. Polymerization shrinkage kinetics and degree of conversion of resin composites. J Oral Sci. 2020 Jun 23;62(3):275-280. doi: 10.2334/josnusd.19-0157. Epub 2020 Jun 4. PMID: 32493864.

149. Braga S, Schettini A, Carvalho E, Shimokawa C, Price RB, Soares CJ. Effect of the Sample Preparation and Light-curing Unit on the Microhardness and Degree of Conversion of Bulk-fill Resin-based Composite Restorations. Oper Dent. 2022 Mar 1;47(2):163-172. doi: 10.2341/20-043-L. PMID: 35604828.

150. Bociong K, Szczesio A, Sokolowski K, Domarecka M, Sokolowski J, Krasowski M, Lukomska-Szymanska M. The Influence of Water Sorption of Dental Light-Cured Composites on Shrinkage Stress. Materials (Basel). 2017 Sep 28;10(10):1142. doi: 10.3390/ma10101142. PMID: 28956844; PMCID: PMC5666948.

151. Zhang D, Mao S, Lu C, Romberg E, Arola D. Dehydration and the dynamic dimensional changes within dentin and enamel. Dent Mater. 2009 Jul;25(7):937-45. doi: 10.1016/j.dental.2009.01.101. Epub 2009 Feb 25. PMID: 19246085; PMCID: PMC2692825.

152. Lohbauer U, Pelka M, Belli R, Schmitt J, Mocker E, Jandt KD, Müller FA. Degree of conversion of luting resins around ceramic inlays in natural deep cavities: a micro-Raman spectroscopy analysis. Oper Dent. 2010 Sep-Oct;35(5):579-86. doi: 10.2341/10-012-L. PMID: 20945750.

153. Perdigao J, Lambrechts P, Van Meerbeek B, Vanherle G, Lopes AL. Field emission SEM comparison of four postfixation drying techniques for human dentin. J Biomed Mater Res. 1995 Sep;29(9):1111-20. doi: 10.1002/jbm.820290911. PMID: 8567709.